SM@LHC 2019 conference
23-26 April 2019, Zurich

Jet and photon production at the LHC

Giuseppe Callea on behalf of the ATLAS and CMS collaboration

University of Glasgow

ATLAS EXPERIMENT

CMS Compact Muon Solenoid

23/04/2019

Motivation

- Test of perturbative QCD (pQCD) predictions

→ Colorless photon used as a probe of the hard partonic interaction

- Constraint on proton PDFs (flavour content when jets are tagged)
- Determination of the strong coupling constant
- Event shapes probe the hadronic final state
- Jet substructure distinguish decay products of heavy particles from gluon/quark showers
- Description of background event kinematics to Higgs production

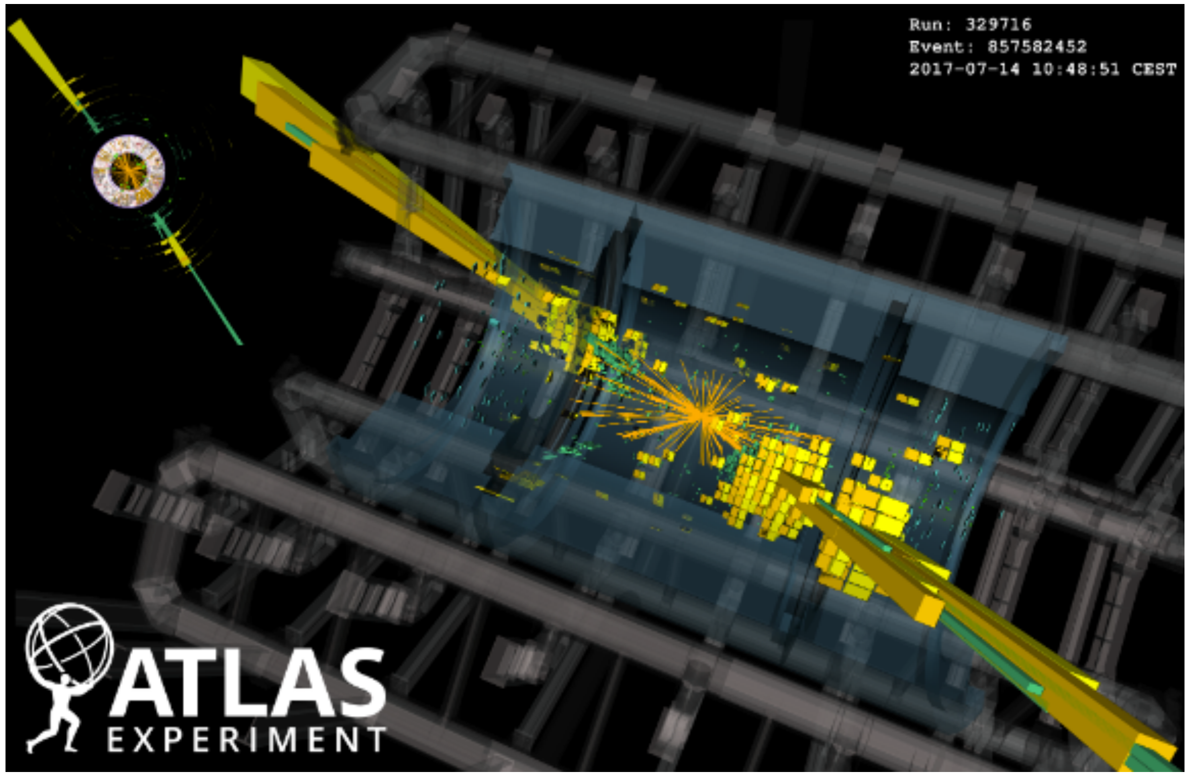

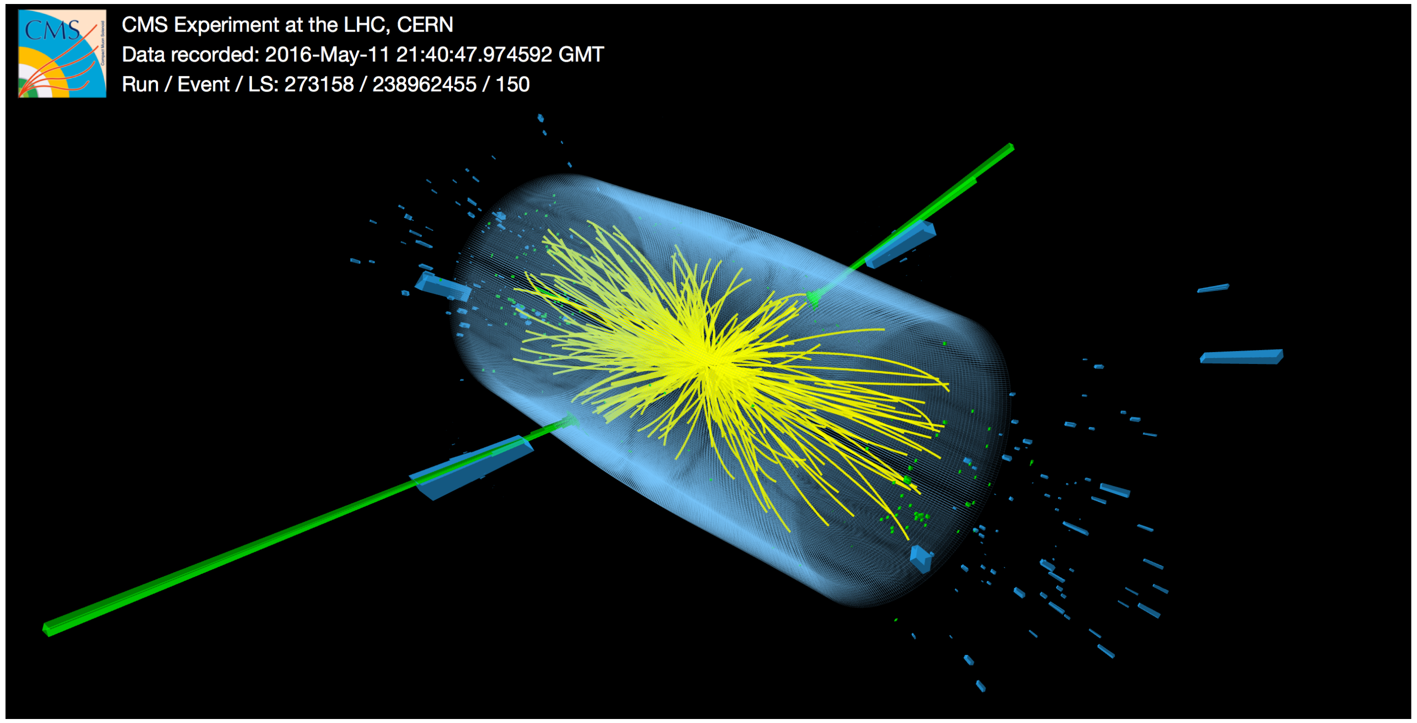

Jets

$\Delta\phi_{12}$ *in nearly back-to-back topologies*

arXiv:1902.04374

Performed in inclusive 2- and 3-jet events: leading and sub-leading jets are required to have $p_{\mathrm{T}} > 100$ GeV and $|y| < 2.5$; a third jet with $p_{\mathrm{T}} > 30$ GeV in the 3-jets case

PH-2J: NLO 2⟶2 calculation

PH-3J (with MiNLO): NLO 2⟶3 calculation

Inclusive 2-jet events

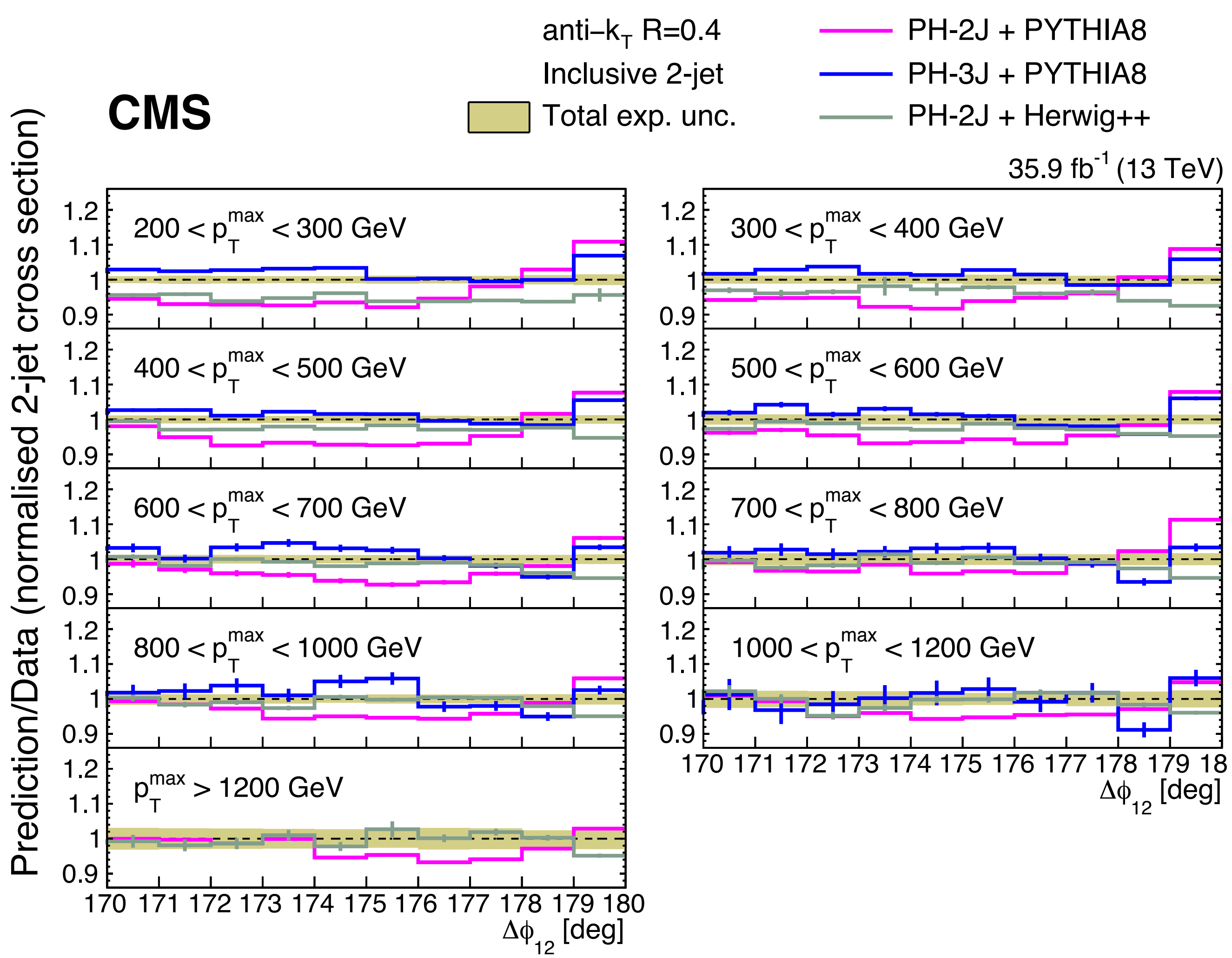

Inclusive 3-jet events

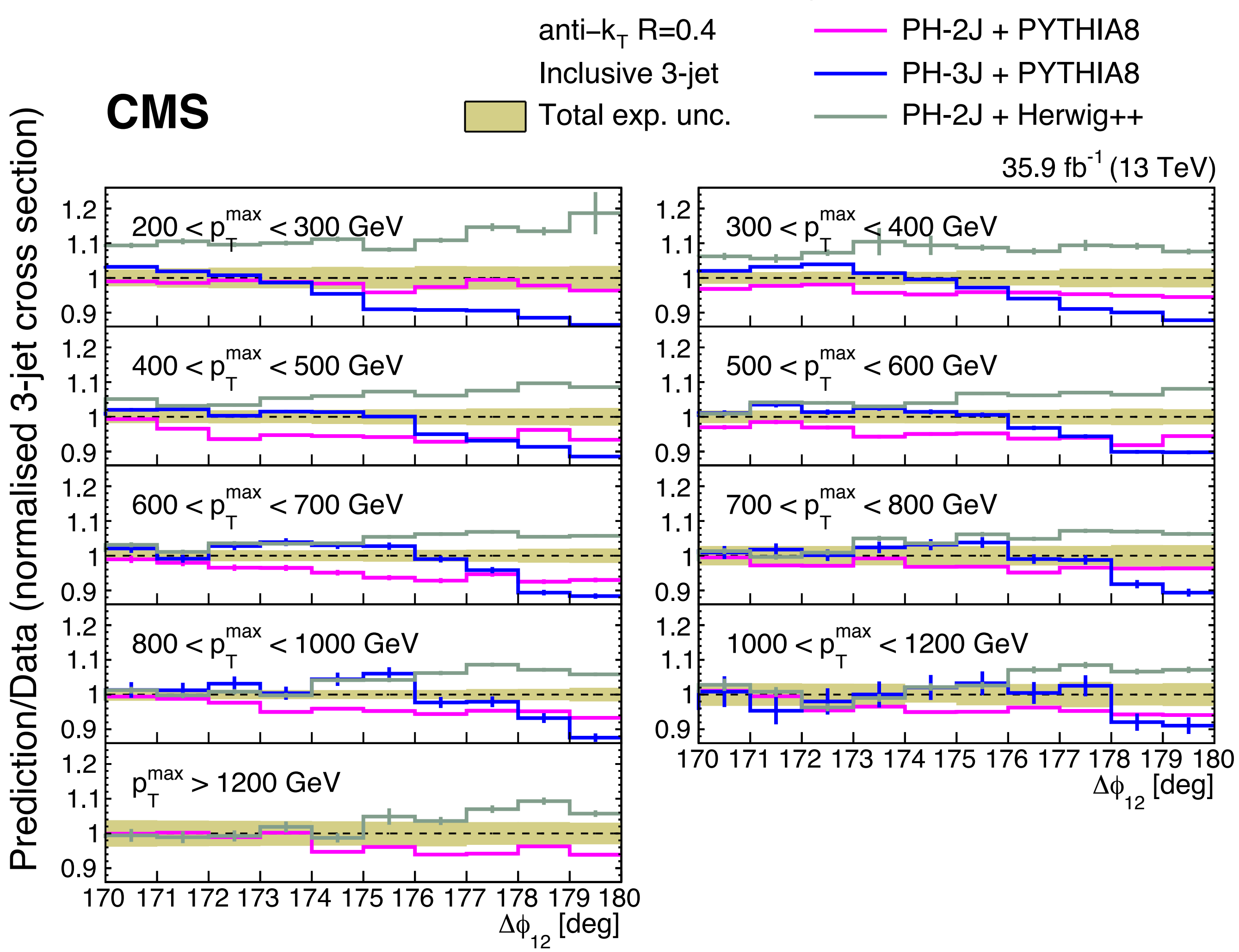

~15% discrepancies between data and the predictions, mainly in $177° < \Delta\phi_{12} < 180°$

Both 2- and 3-jet measurements are not simultaneously described by any model

Azimuthal correlations in 2-, 3- and 4-jet events

EPJC 78 (2018) 566

Measurement as a function of the minimum azimuthal angle between any of the 3 or 4 leading jets ($\Delta\phi_{2j}^{min}$)

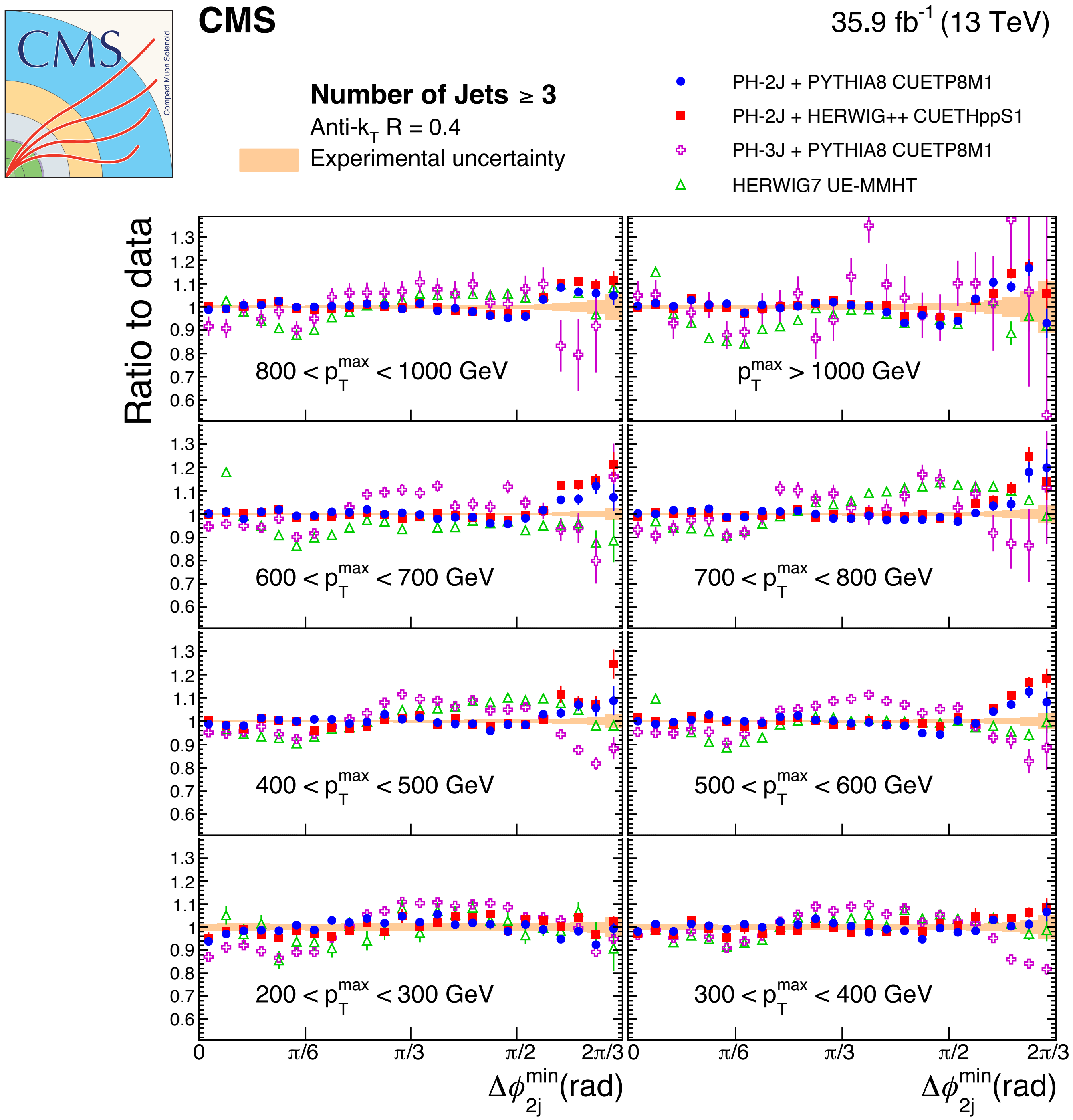

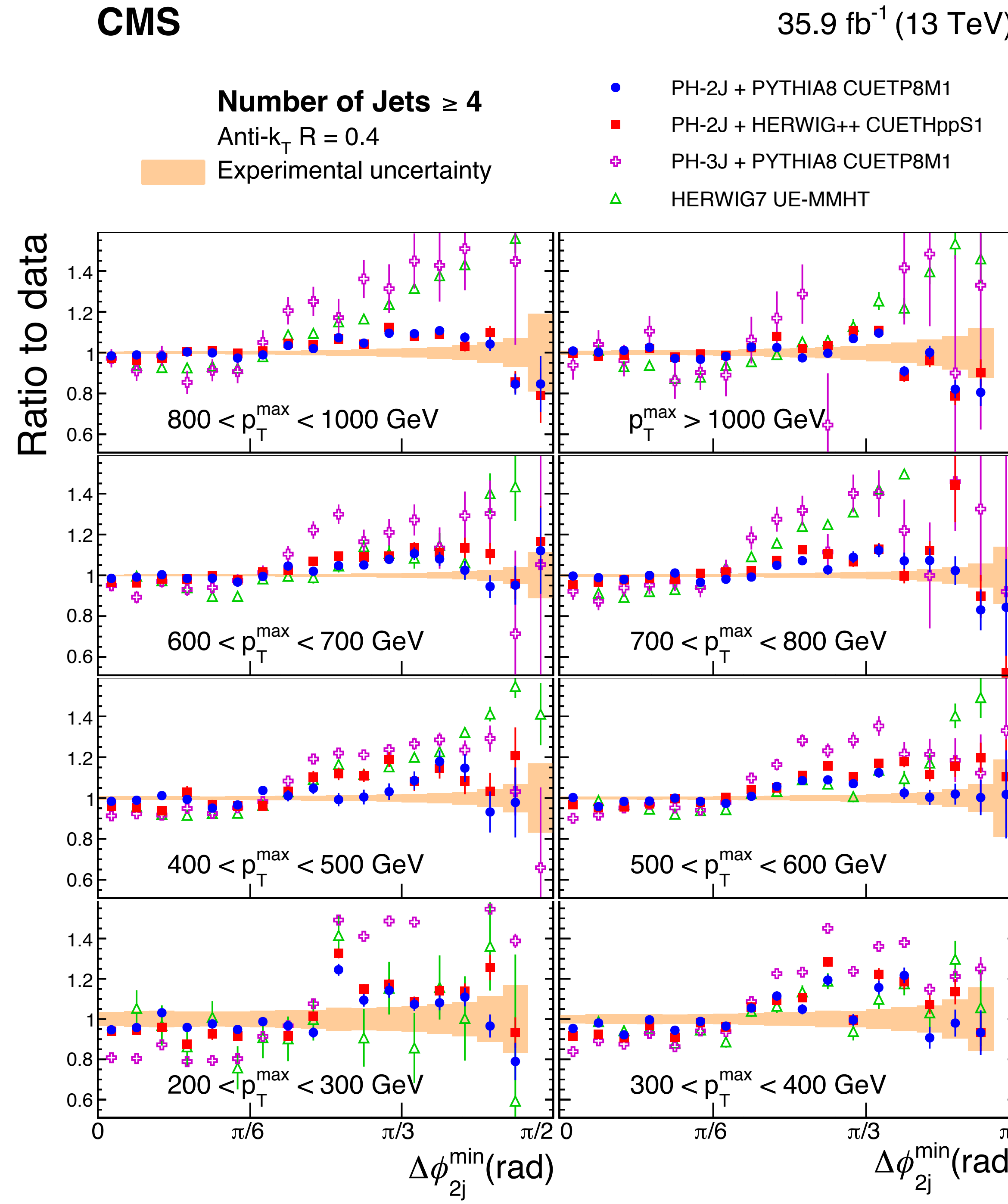

PH-2j matched to Pythia8 or to Herwig++ provides the best description of the measurements

Dijet azimuthal decorrelation

Phys. Rev. D 98 (2018) 092004

- Measurement of the y and p_T dependence of the dijet azimuthal decorrelations using the fraction of inclusive jet events with $\Delta\phi < \Delta\phi_{max}$ ($R_{\Delta\phi}$)
- $R_{\Delta\phi}$ is measured as a function of y^*, $H_\mathrm{T} = (p_{\mathrm{T},1} + p_{\mathrm{T},2})/2$ and $\Delta\phi_{max}$

Variable	Value
$p_{\mathrm{T}\min}$	100 GeV
$y_{\mathrm{boost}}^{\max}$	0.5
$y_{\max}^*$	2.0
$p_{\mathrm{T}1}/H_\mathrm{T}$	$> 1/3$

Good agreement between data and the theoretical predictions of NLOJET++ within uncertainties.

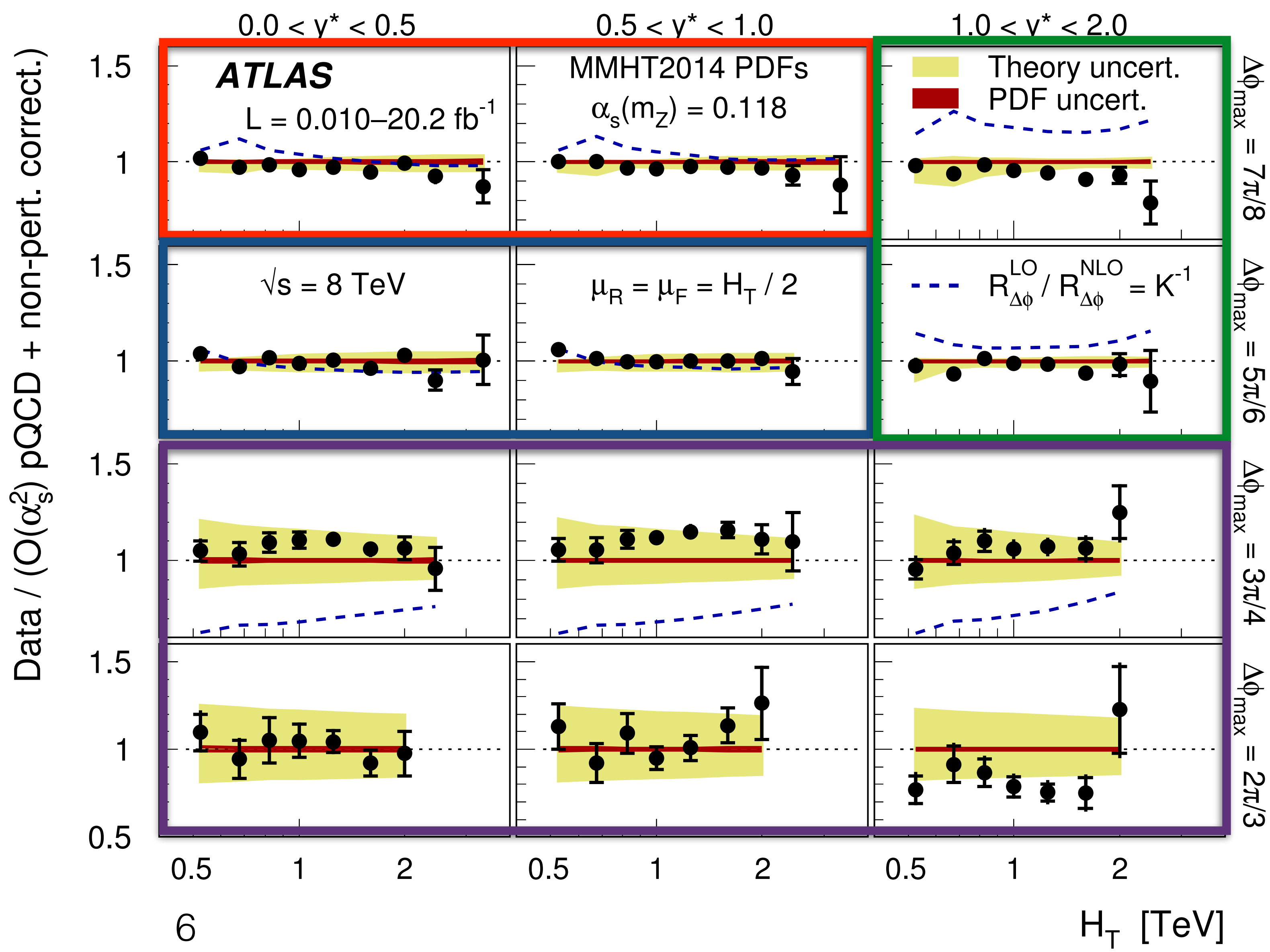

For the α_s measurement:

- $\Delta\phi_{max} = 2\pi/3$ and $3\pi/4$ are rejected for the large scale dependence
- $1 < y^* < 2$ region is rejected due to the large NLO corrections
- $\Delta\phi_{max} = 5\pi/6$ and $7\pi/8$ are the best choices
- $\Delta\phi_{max} = 7\pi/8$ region is chosen

Determination of α_S

$\alpha_S(m_Z)$	Total uncert.	Statistical	Experimental correlated	Non-perturb. corrections	MMHT2014 uncertainty	PDF set	$\mu_{R,F}$ variation
0.1127	$^{+6.3}_{-2.7}$	± 0.5	$^{+1.8}_{-1.7}$	$^{+0.3}_{-0.1}$	$^{+0.6}_{-0.6}$	$^{+2.9}_{-0.0}$	$^{+5.2}_{-1.9}$

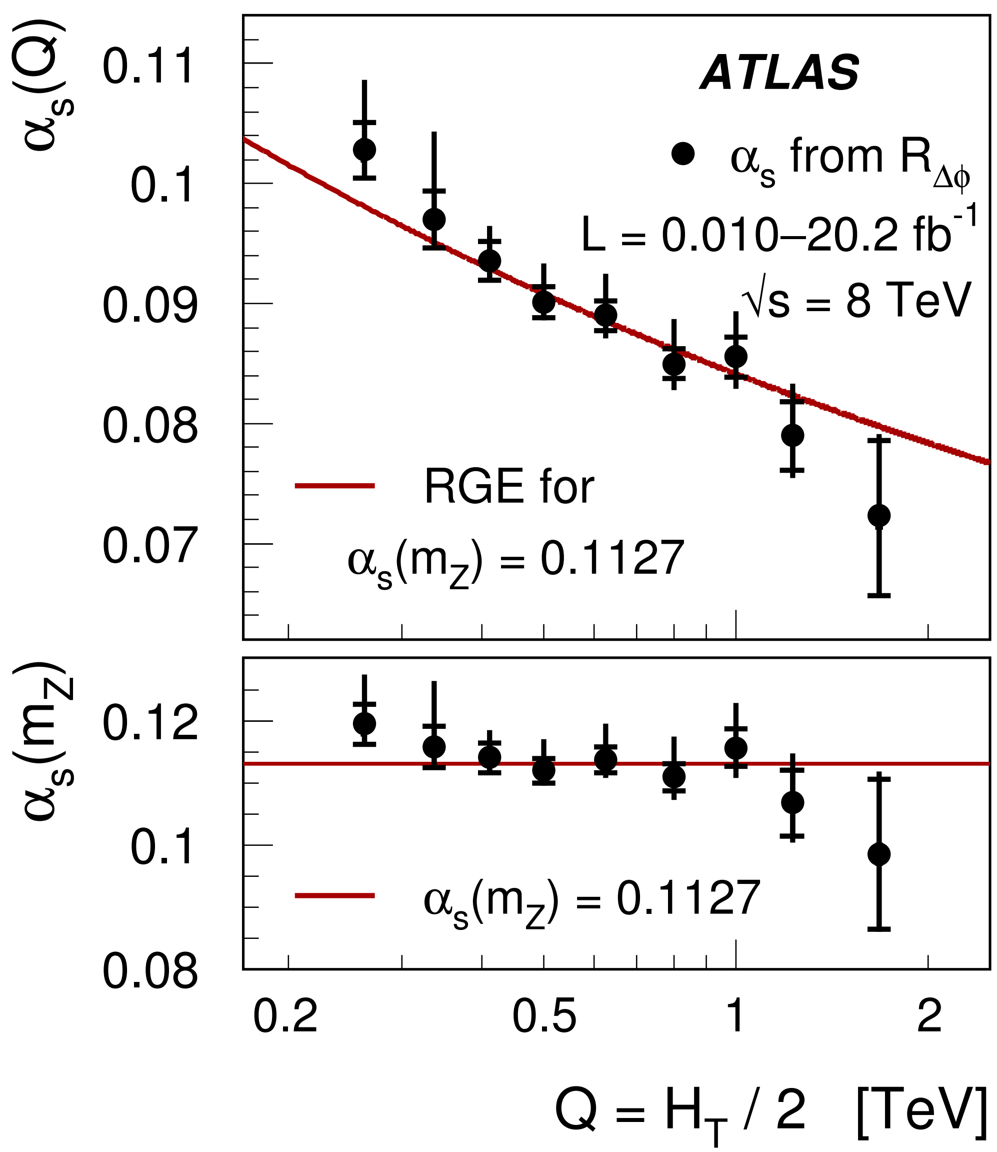

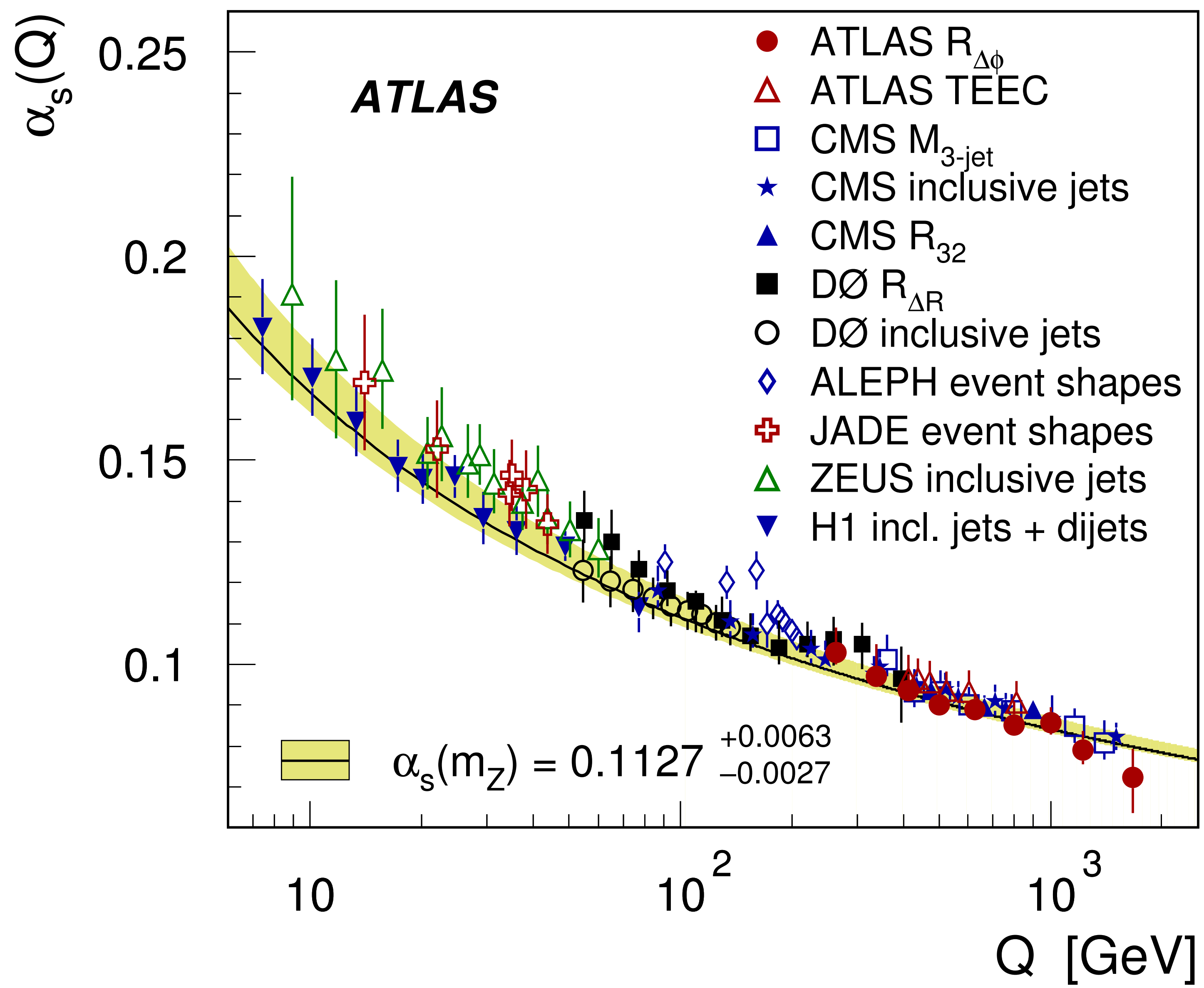

Good agreement with the world average value (PDG)

Event shape variables in multijet final states

JHEP 12 (2018) 117

Sensitive to the flow of energy in hadronic final states

Complement of transverse thrust ($\tau_\perp$): $\tau_\perp \equiv 1 - T_\perp \quad T_\perp \equiv \max_{\hat{n_T}} \frac{\sum_i |\vec{p}_{T,i} \cdot \hat{n_T}|}{\sum_i \vec{p}_{T,i}}$

Total jet broadening (B_{TOT})

Measured in different $H_{T,2}$ bins

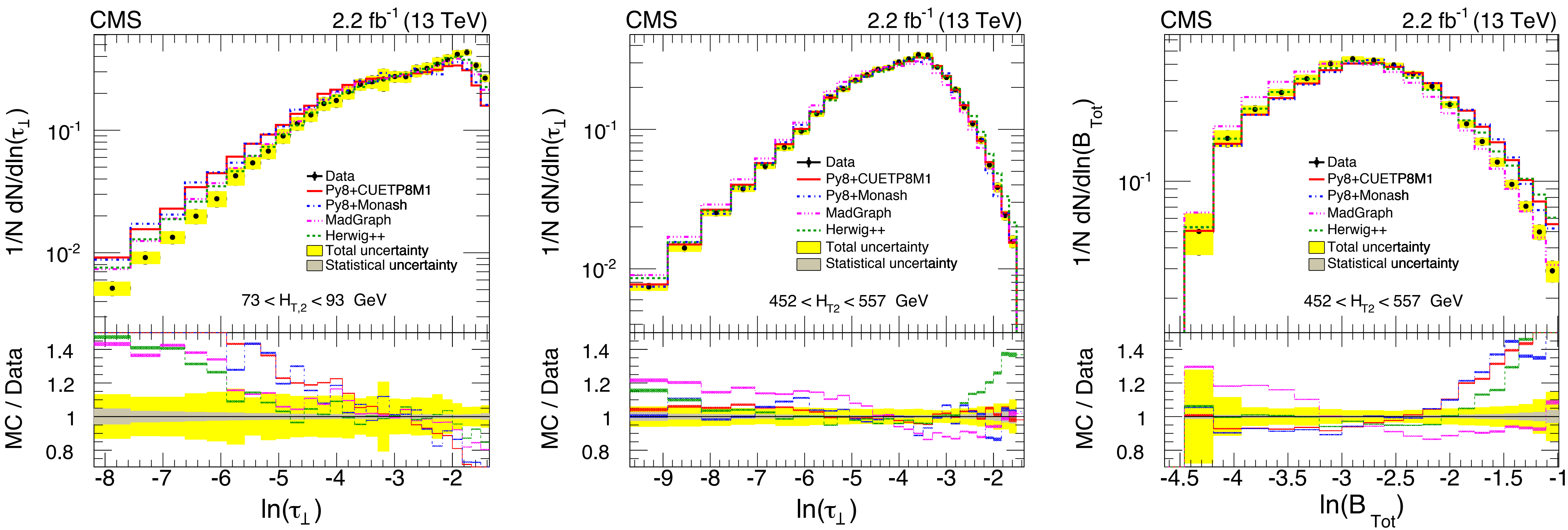

The general agreement improves as $H_{T,2}$ increases

Pythia gives the best description of $\tau_\perp$, while both Herwig and Madgraph are in better agreement with the data in the case of $B_{TOT} \rightarrow$ Energy flow in transverse plane described well by string fragmentation and p_T ordered showers, while cluster fragmentation and angular-ordered shower better describe the out of plane energy flow

Measurement of the jet substructure observables

Jet substructure observables in $t\bar{t}$ and inclusive jet events **arXiv:1903.02942**

anti-kt (R=1) jets groomed using 2 different techniques: trimming and soft drop (SD)

The observables measured are sensitive to pronged substructure and can be used for tagging jets from boosted massive particles

Normalised energy correlation function and ratios

$$e_2^\beta = \frac{1}{p_T^2} \sum_{i<j} p_{Ti} p_{Tj} R_{ij}^\beta \qquad e_3^\beta = \frac{1}{p_T^3} \sum_{i<j<k} p_{Ti} p_{Tj} p_{Tk} R_{ij}^\beta R_{ik}^\beta R_{jk}^\beta$$

Ratio of energy correlation function: $D_2^{(\beta)} = e_3^{(\beta)} / \left(e_2^{(\beta)}\right)^3$

Dijet selection

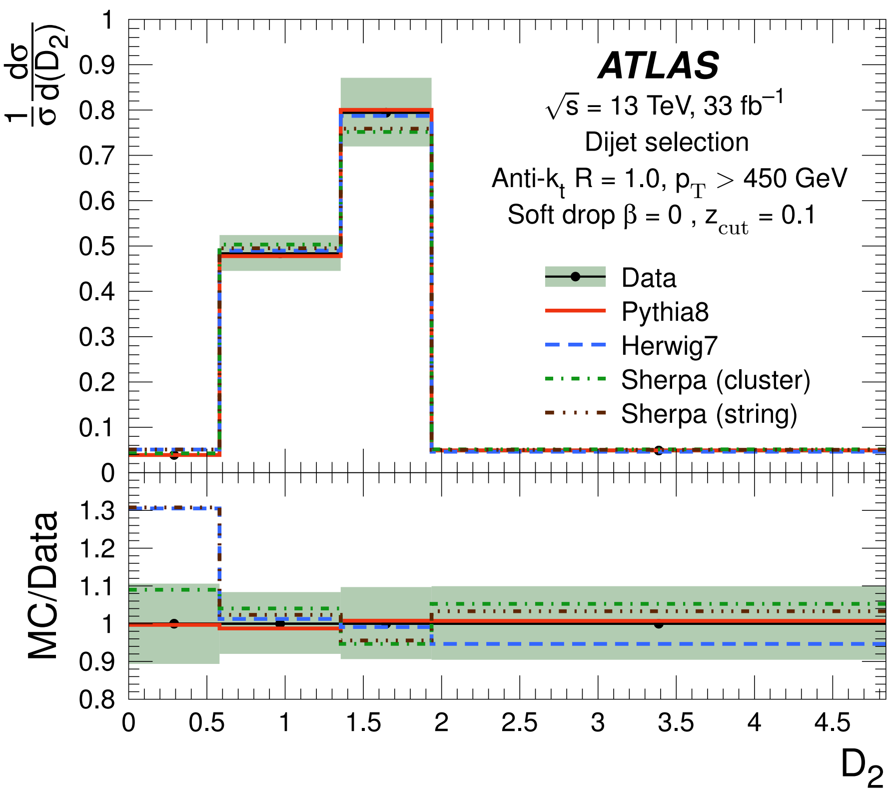

Top selection

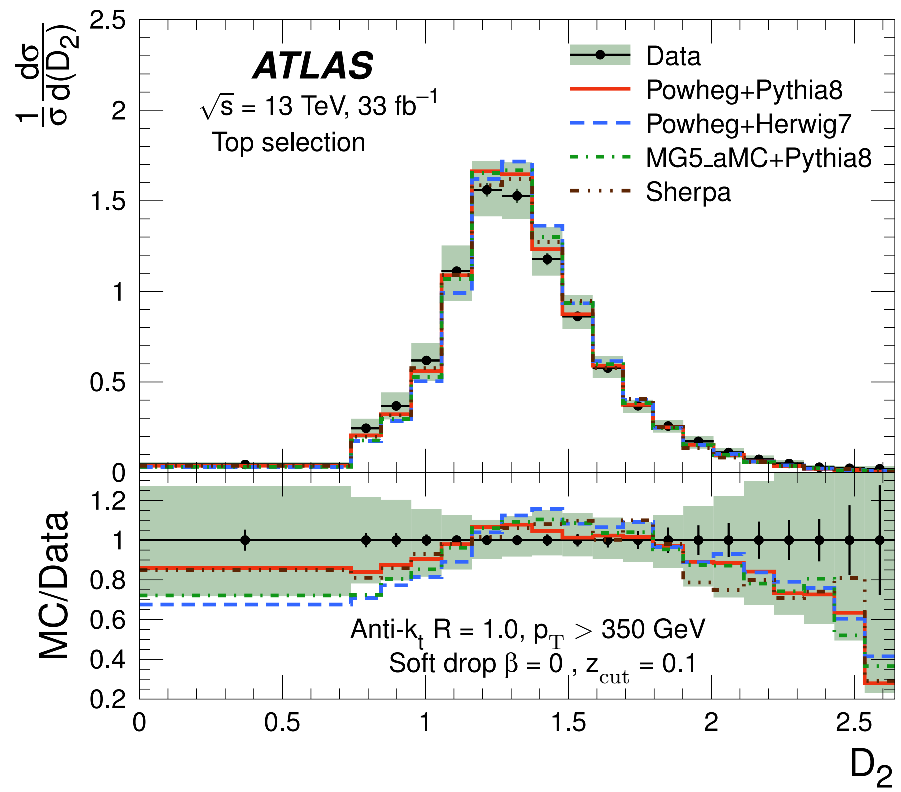

W selection

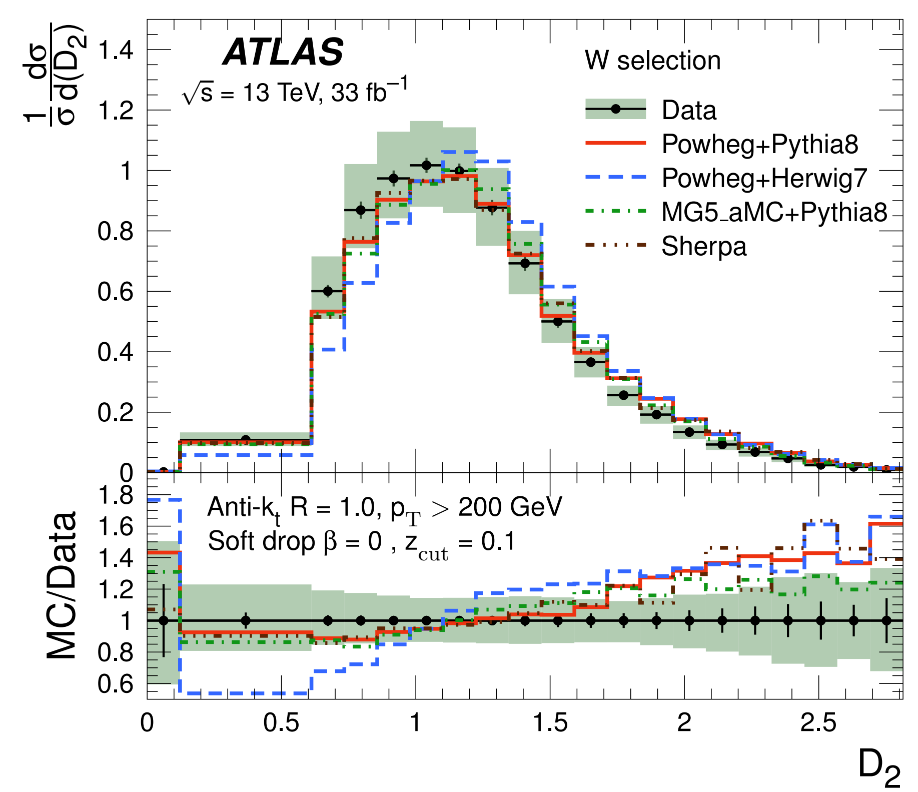

Good data/MC agreement in the dijet and top selection

In the W selection all the predictions have a shifted peak relative to data ⟶ Models overestimating the gluon radiation for the D2 observables

Gluon splitting into $b\bar{b}$

Phys. Rev. D 121 (2018) 092001

Properties of $g \rightarrow b\bar{b}$ in the high-p_T small angles regime

Main background source in analyses involving boosted Higgs decaying into b-quark pairs

anti-kt (R=0.2) track jets are ghost matched to anti-kt (R=1) trimmed jets

Those large-R jets which do not contain two B-hadrons track jets are subtracted using template fits

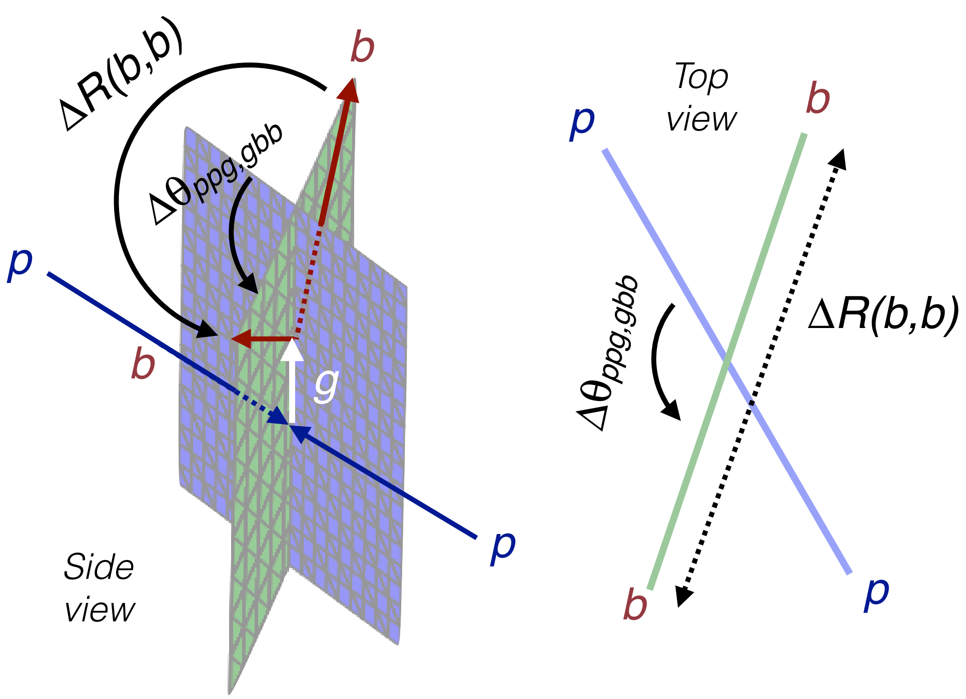

Deviations in the data/MC (LO Sherpa and Pythia) comparison are observed

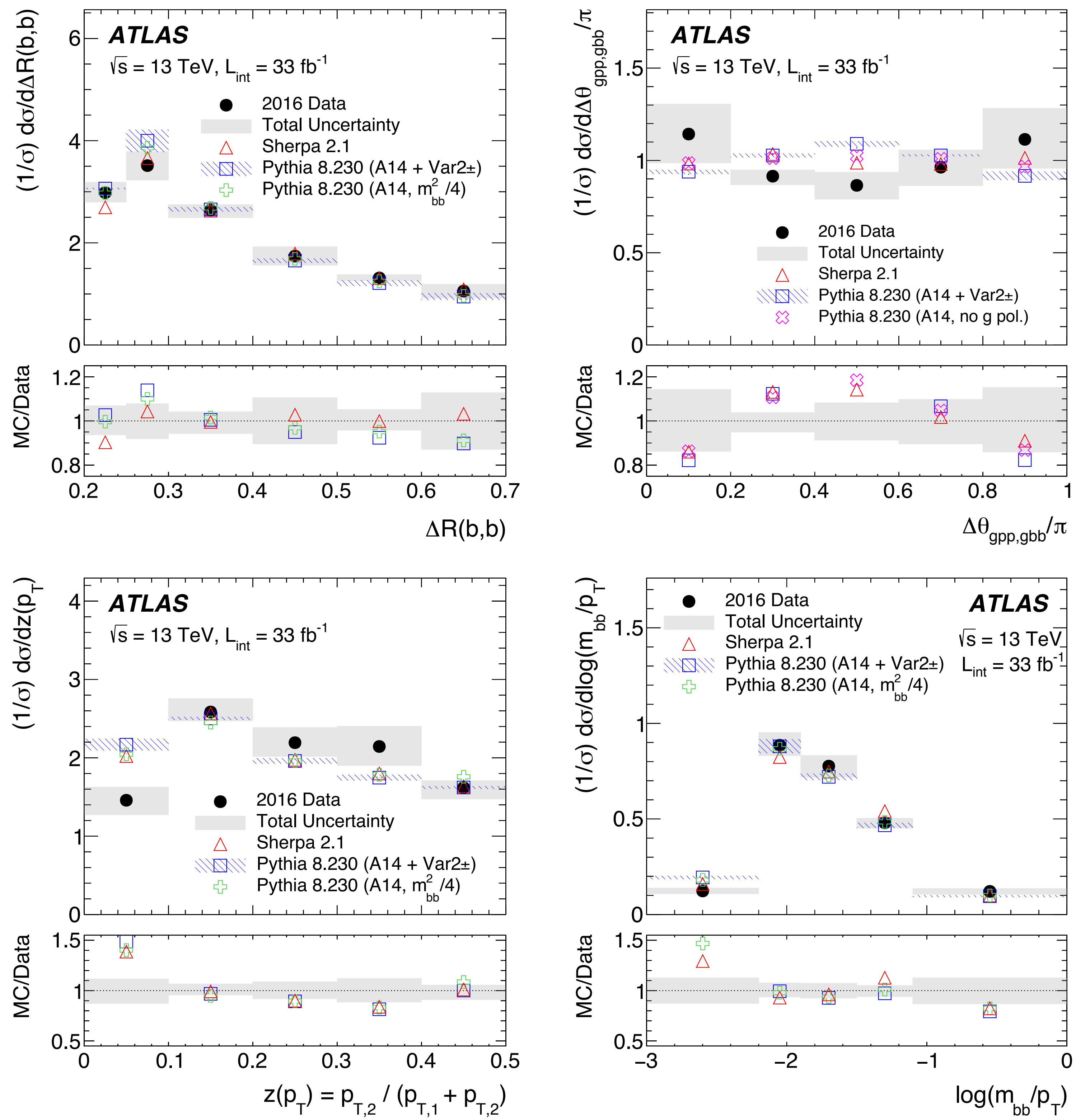

Jet mass cross section in dijet events

JHEP 11 (2018) 113

Measured in dijet events with and without a jet grooming algorithm (SD), in bins of p_T

Sensitive to the jet internal structure and governed by QCD radiation: gluon radiation (hard), pileup and UE (soft)

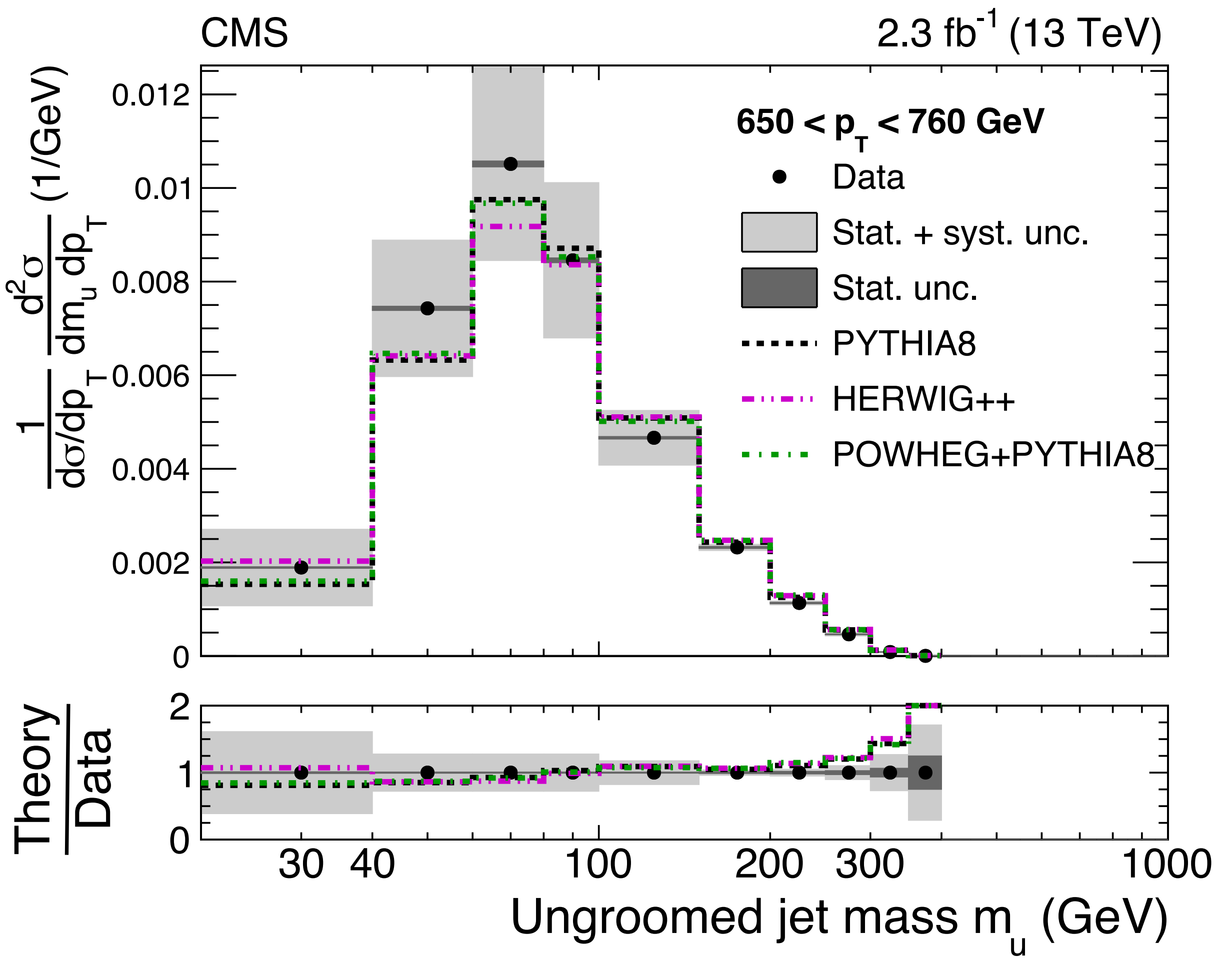

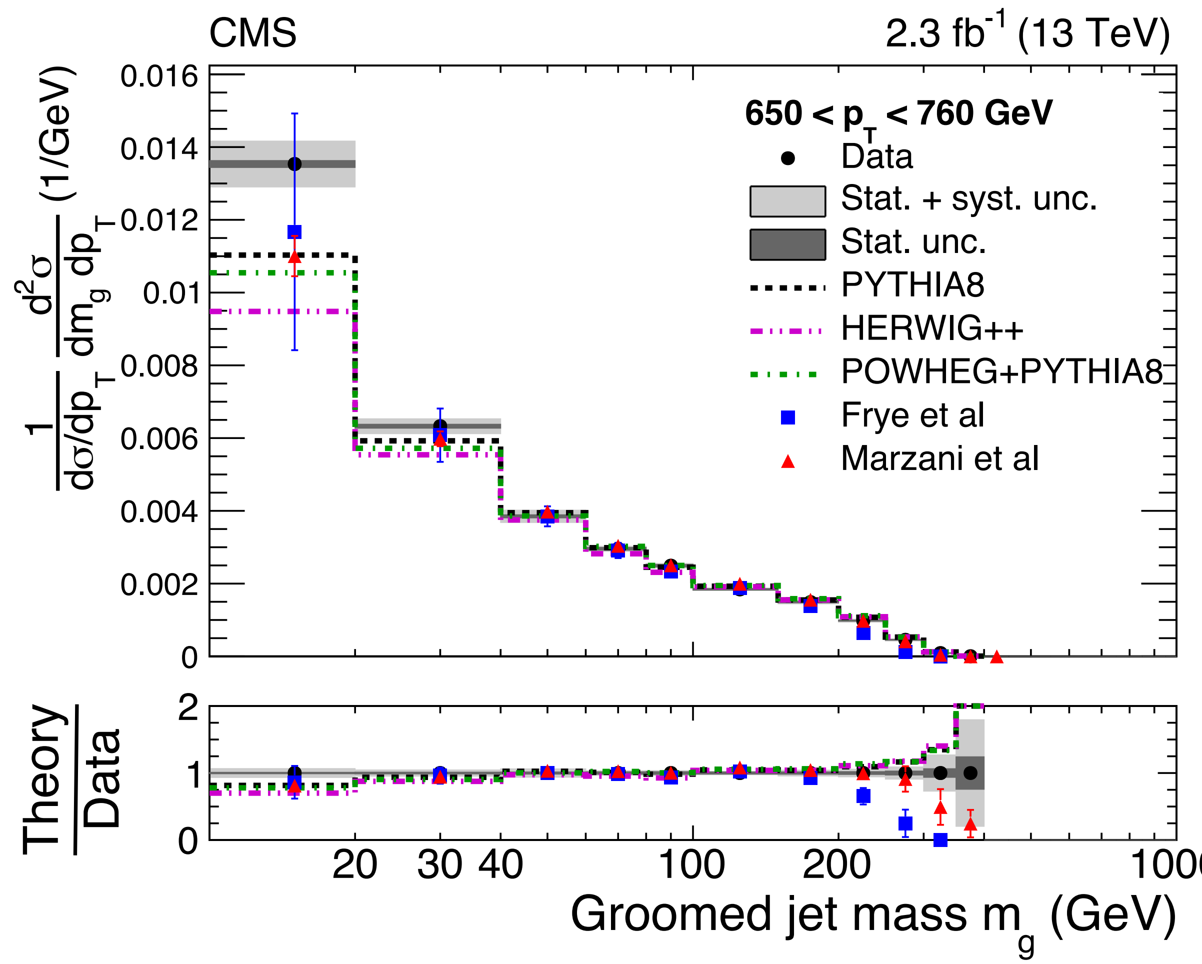

The use of the grooming algorithm decreases the value of the jet mass and reduces the sensitivity to the different details of the physics modelling and PU effects

Significant uncertainties reduction at low mass values in the groomed jet case

Theoretical predictions including resummation are in good agreement with the data within the uncertainties

Photons

Prompt photons ⟶ Photons not coming from hadron decays

Direct

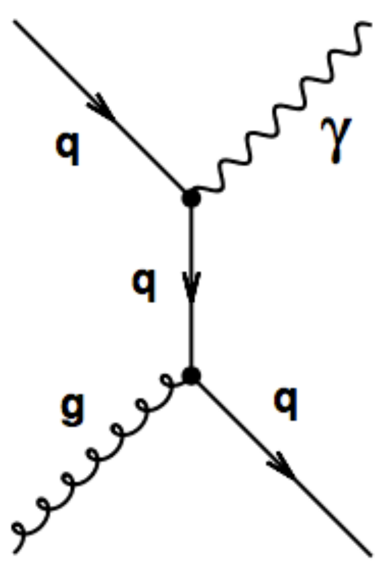

Fragmentation

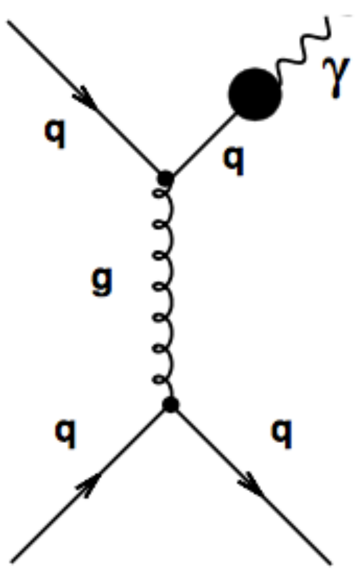

Photon + jet at 13 TeV Phys. Lett. B 780 (2018) 578

Measurements of differential cross sections as a function of E_T^{γ}, p_T^{jet}, $\Delta\phi^{\gamma-jet}$, $m^{\gamma-jet}$

$\cos\theta^* = \tanh\,(\eta^{\gamma} - y^{jet})/2$ (θ^* coincides with the scattering angle in the CM frame)

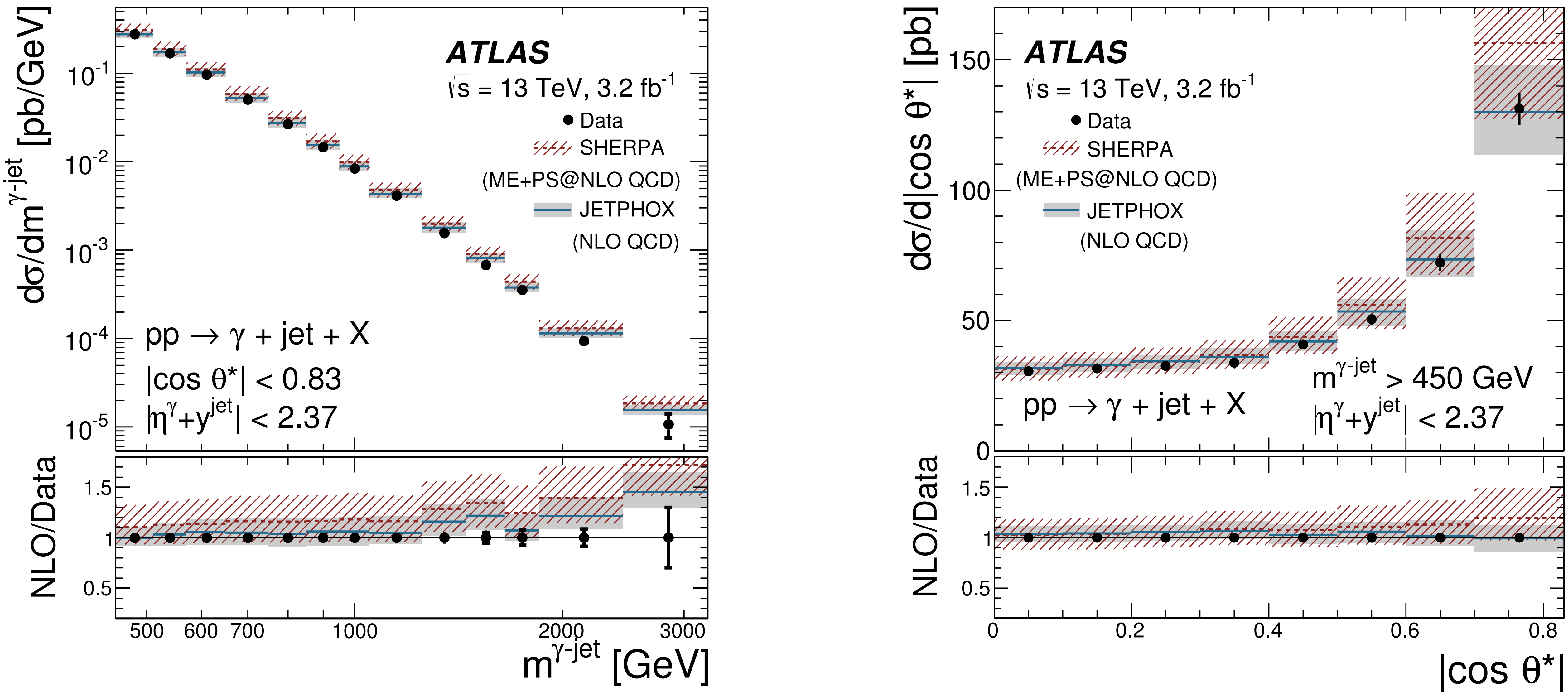

The QCD predictions of Jetphox and ME+PS@NLO Sherpa give an adequate description of the data within the theoretical uncertainties

$d\sigma/d|\cos\theta^*|$ increases as $|\cos\theta^*|$ increases, in agreement with the NLO expectations

Photon + jet at 13 TeV

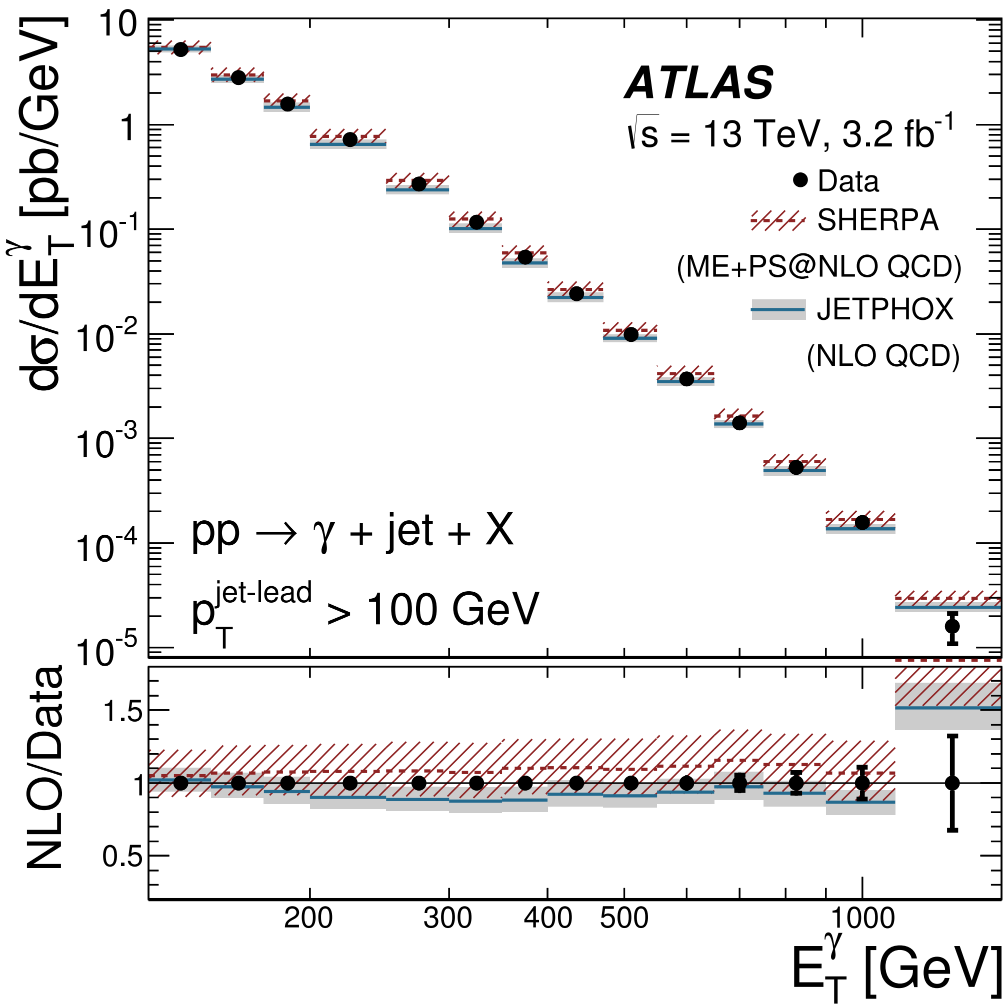

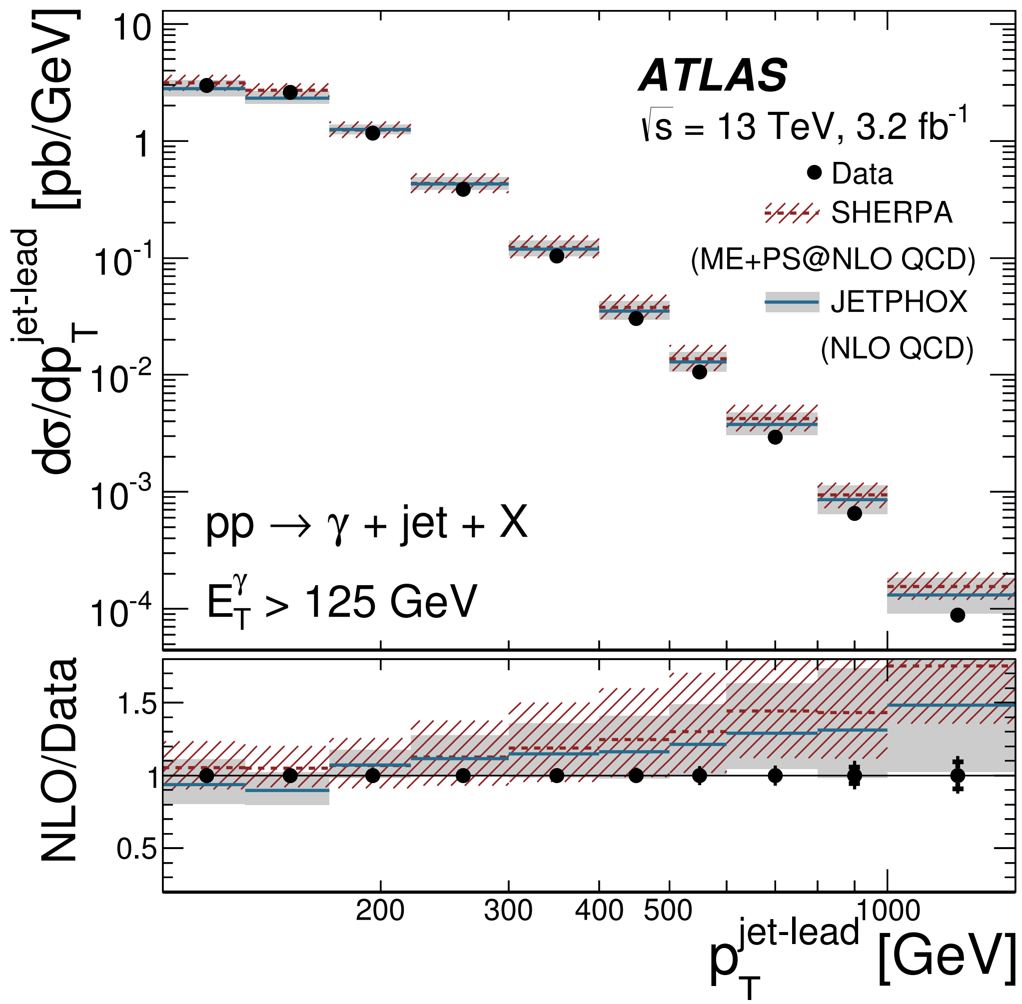

$d\sigma/d|\cos\theta^*|$ is expected to behave as:

- $(1-|\cos\theta^*|)^{-1}$ for the direct process
- $(1-|\cos\theta^*|)^{-2}$ for the fragmentation process

when $|\cos\theta^*| \to 1$

The data shape is closer to that of the direct contribution. Consistent with the dominance of processes in which the exchanged particle is a quark

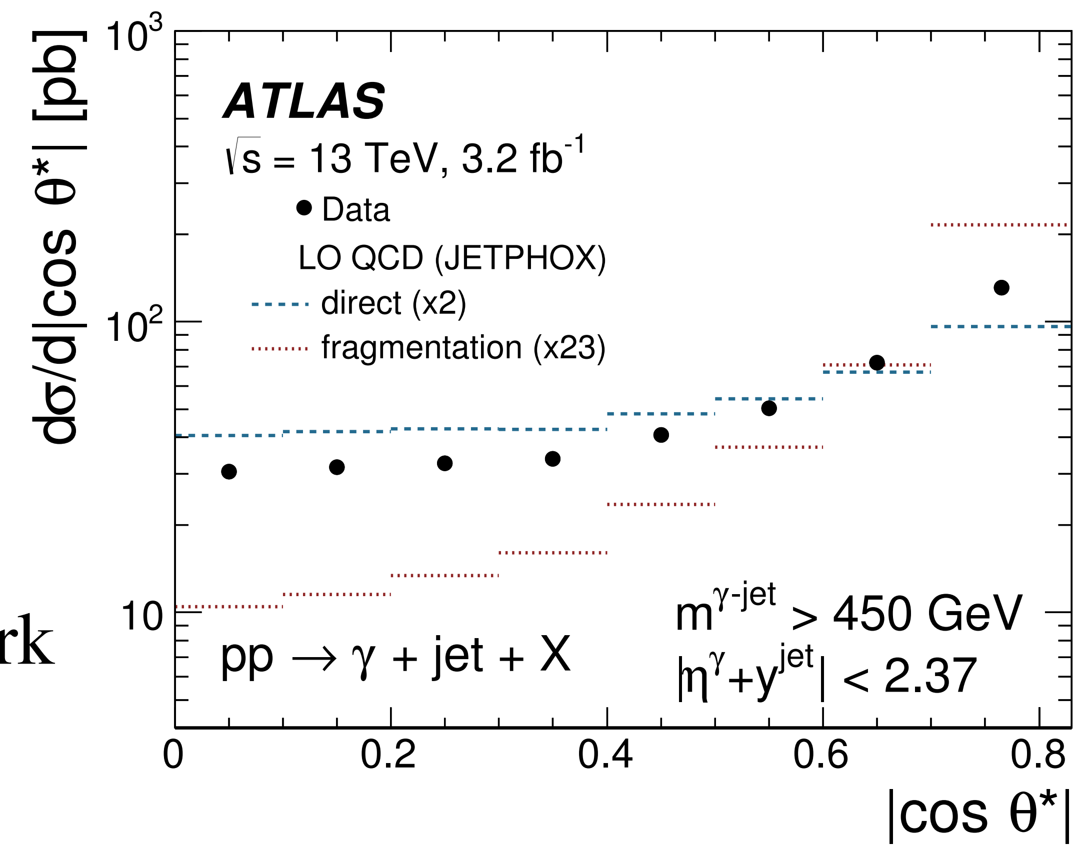

Inclusive photon and γ+ jet at 13 TeV

EPJC 79 (2019) 20

Inclusive (+jet) cross sections are measured as a function of E_T^{γ} and $|\eta^{\gamma}|$ (and $|y^{jet}|$)

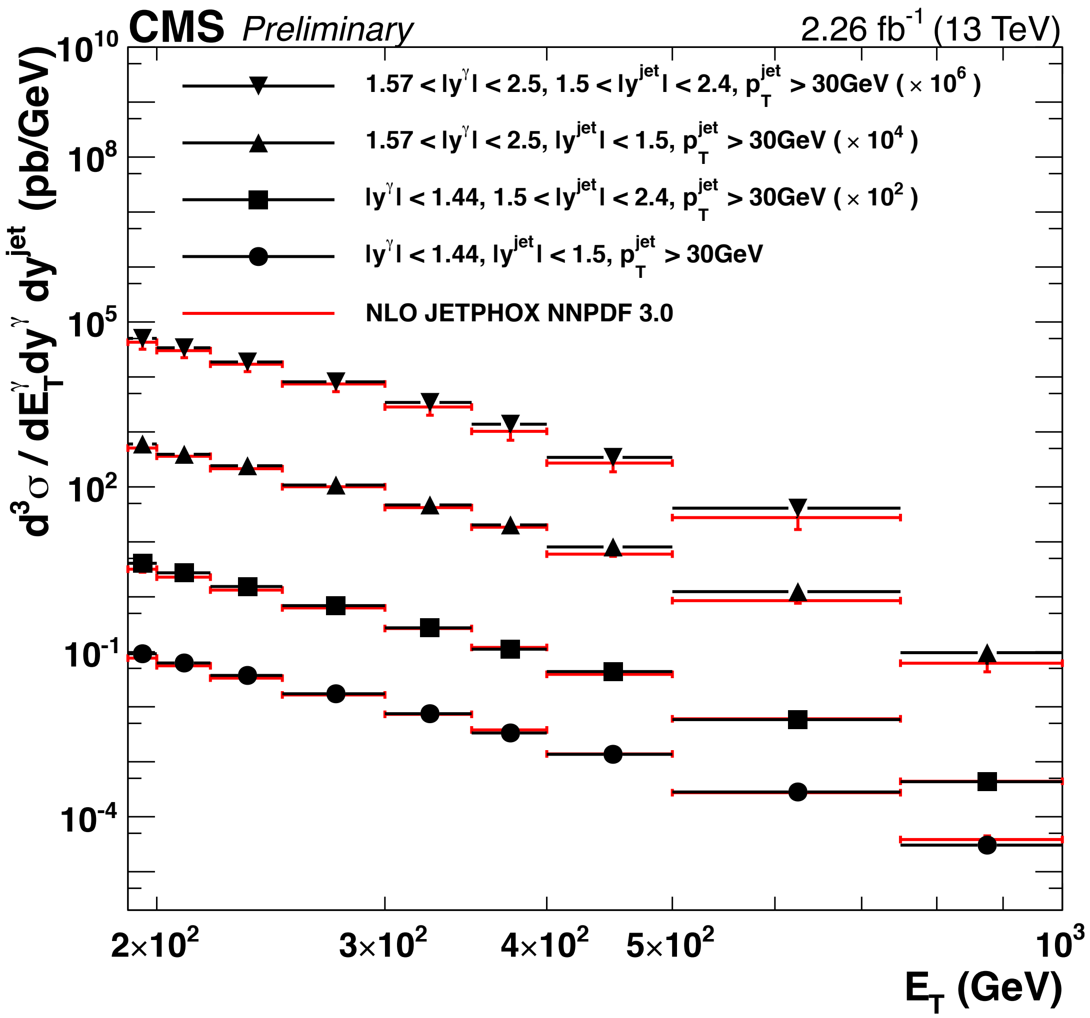

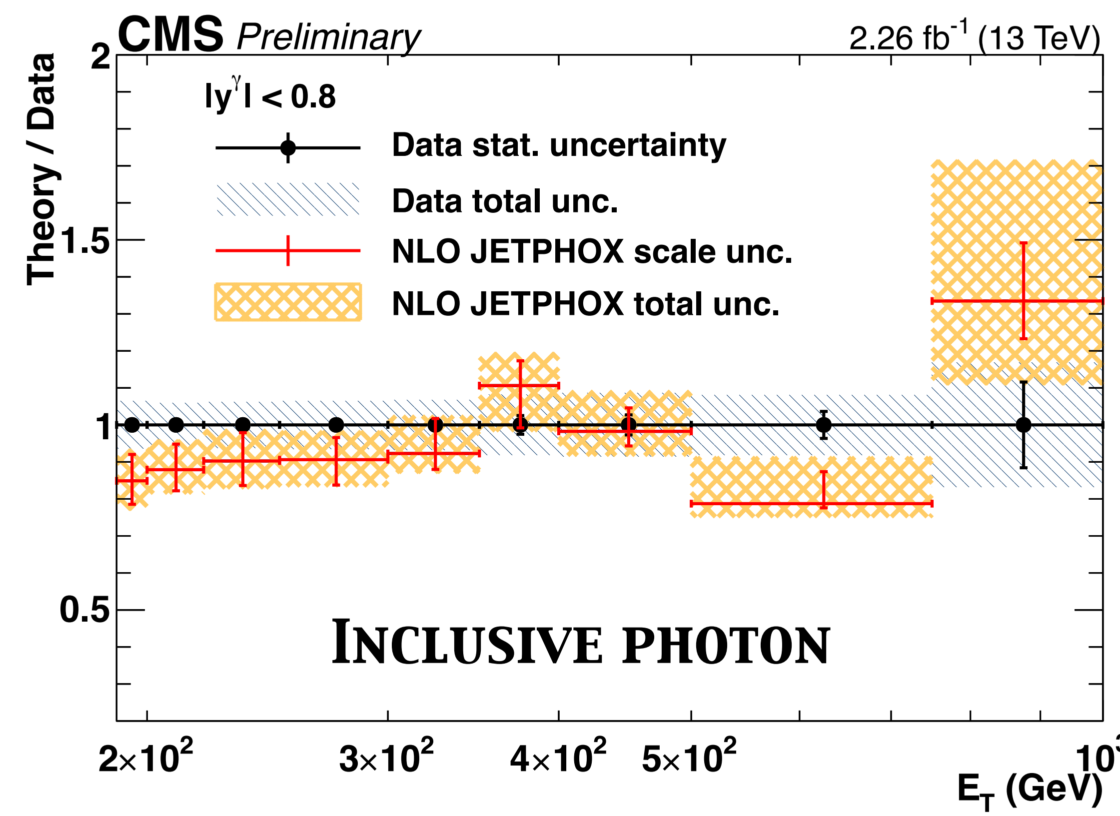

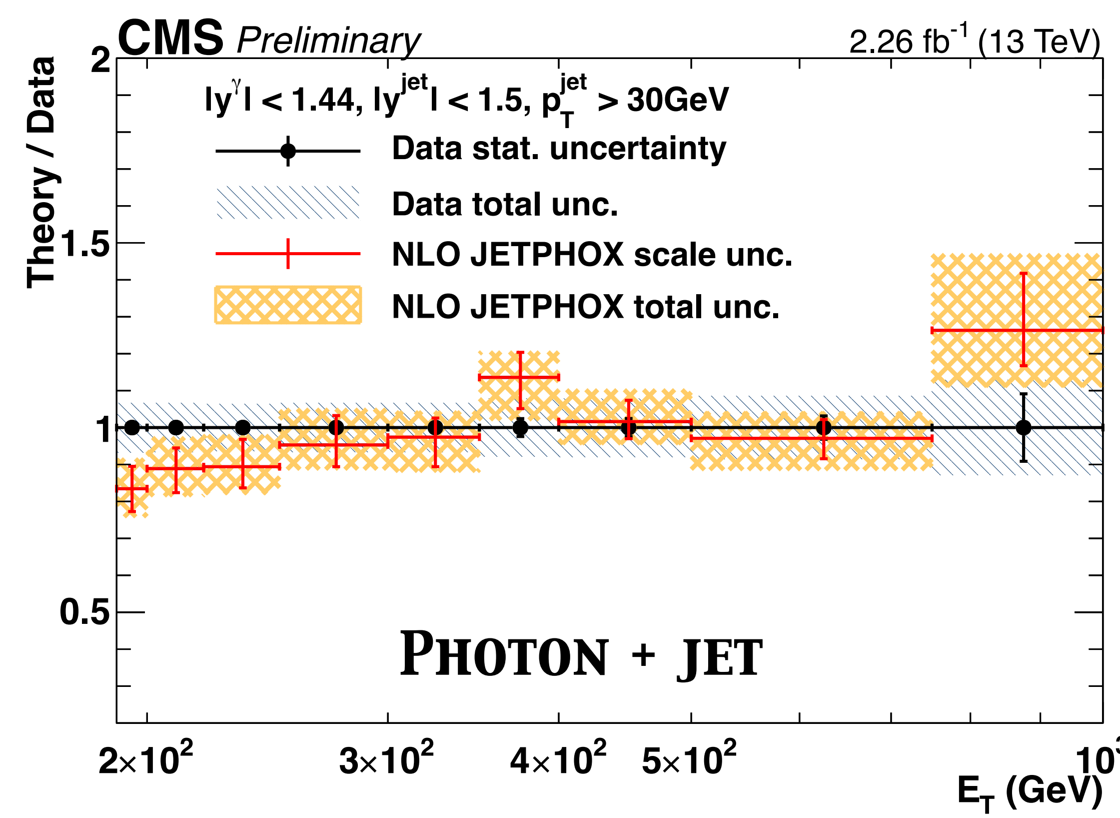

Photon identification made using a boosted decision tree algorithm

Both measurements are in good agreement with the NLO pQCD predictions of Jetphox within uncertainties

Ratio of photon cross sections at 8 and 13 TeV

arXiv:1901.10075

Ratio ($R^{\gamma}_{13/8}$) measured as a function of E_T^{γ} in different $|\eta^{\gamma}|$ ranges. Accounts for the correlation between uncertainties: stringent test of pQCD with an hard colorless probe

Theoretical

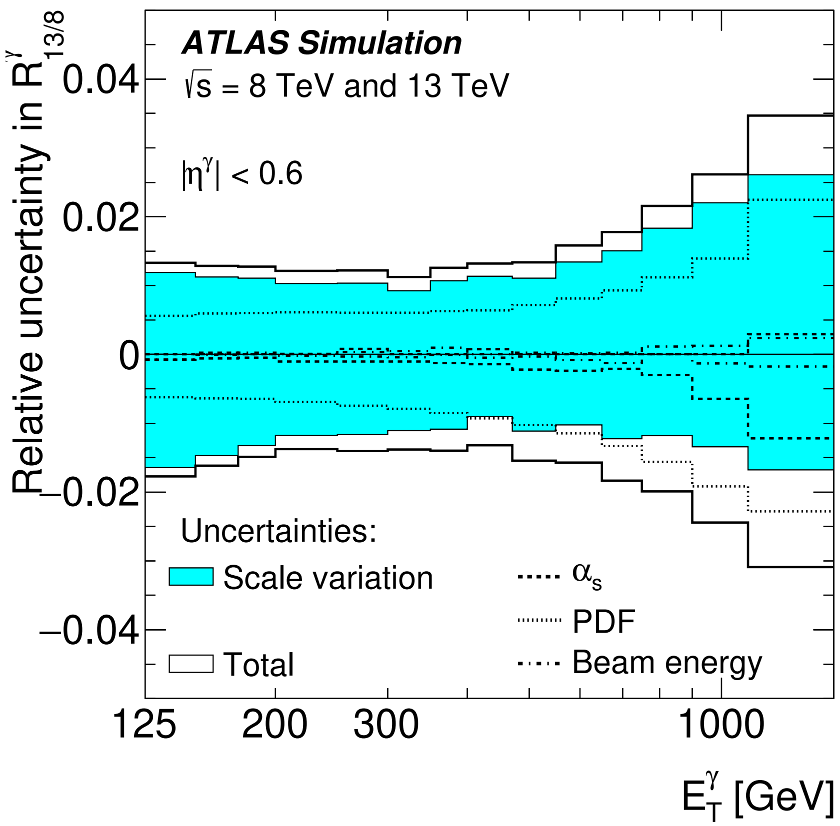

Experimental

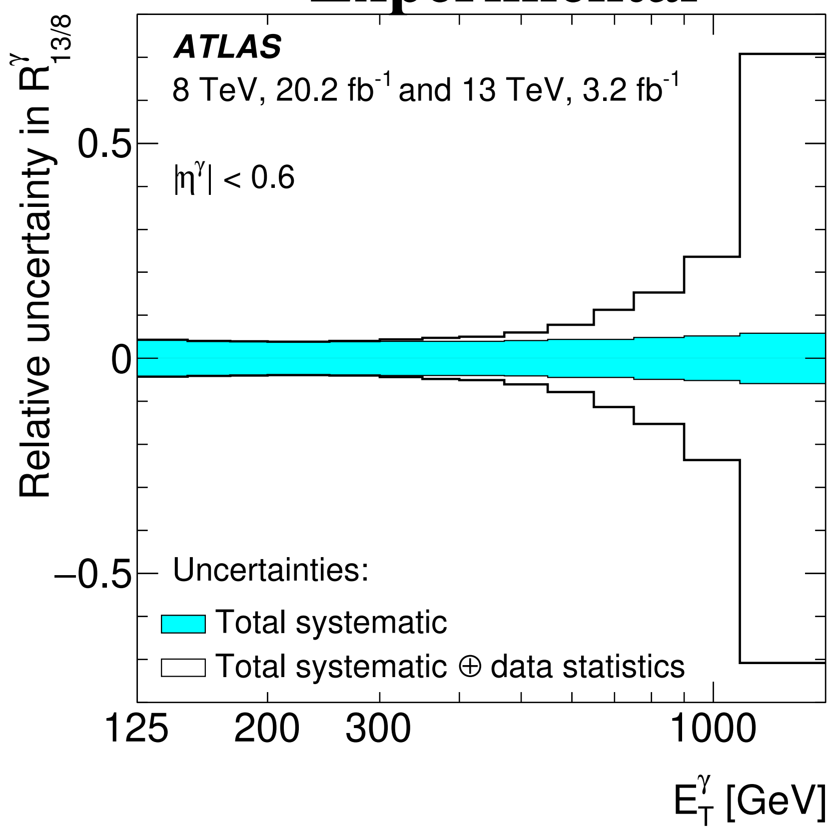

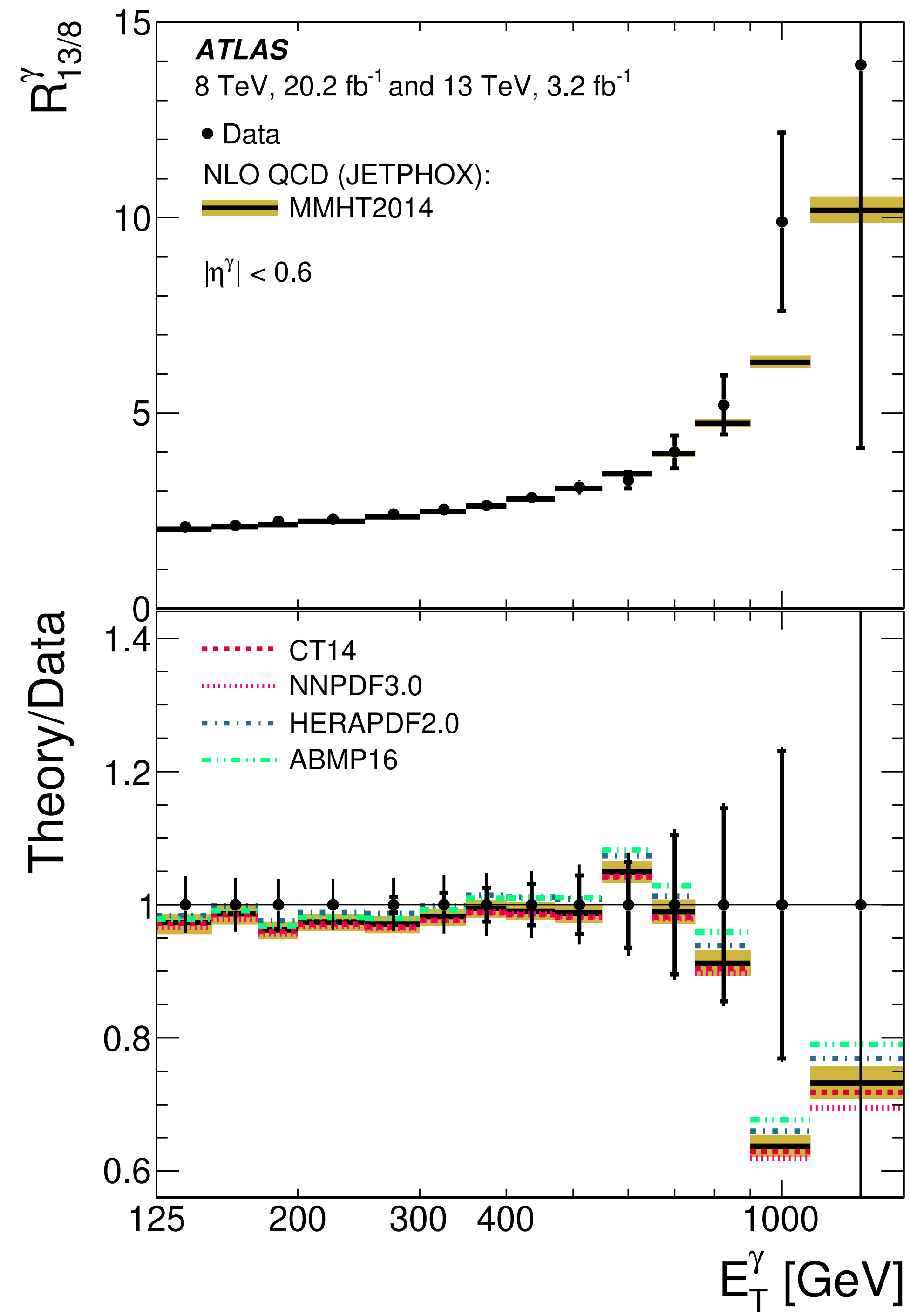

Significant reduction in both experimental and theoretical uncertainties (photon energy scale no longer the dominant unc.)

NLO pQCD calculation of Jetphox with different PDF sets in good agreement with the data

Validation of evolution of isolated photon production in pp collisions from $\sqrt{s}$ = 8 to 13 TeV

Summary and Conclusions

Many great results from ATLAS and CMS

Most of these results are well modeled by the predictions

Although some discrepancies were observed → need to improve the MC event simulation and pQCD predictions

Useful results for tuning Monte Carlo models

Many advances in theoretical predictions recently (NNLO), which can be compared to the high-precision model-independent ATLAS and CMS measurements (**eg. arXiv:1904.01044v1**)

Great effort to reduce experimental systematic uncertainties with respect to the previous measurements

THANK YOU FOR YOUR ATTENTION!

Backup

$\Delta\phi_{12}$ *in nearly back-to-back topologies*

Monte Carlo event generators, parton densities, and underlying event tunes used for comparison with measurements

Matrix element generator	Simulated diagrams	PDF set	Tune
PYTHIA 8.219 [10]	2→2 (LO)	NNPDF2.3LO [15, 16]	CUETP8M1 [14]
HERWIG++ 2.7.1 [11]	2→2 (LO)	CTEQ6L1 [17]	CUETHppS1 [14]
MADGRAPH [18, 19]+ PYTHIA 8.219 [10]	2→2, 2→3, 2→4 (LO)	NNPDF2.3LO [15, 16]	CUETP8M1 [14]
PH-2J [20–22] + PYTHIA 8.219 [10]	2→2 (NLO)	NNPDF3.0NLO [23]	CUETP8M1 [14]
PH-2J [20–22] + HERWIG++ 2.7.1 [11]	2→2 (NLO)	NNPDF3.0NLO [23]	CUETHppS1 [14]
PH-3J [20–22] + PYTHIA 8.219 [10]	2→3 (NLO)	NNPDF3.0NLO [23]	CUETP8M1 [14]

$\Delta\phi_{12}$ *in nearly back-to-back topologies*

Inclusive 2-jet events

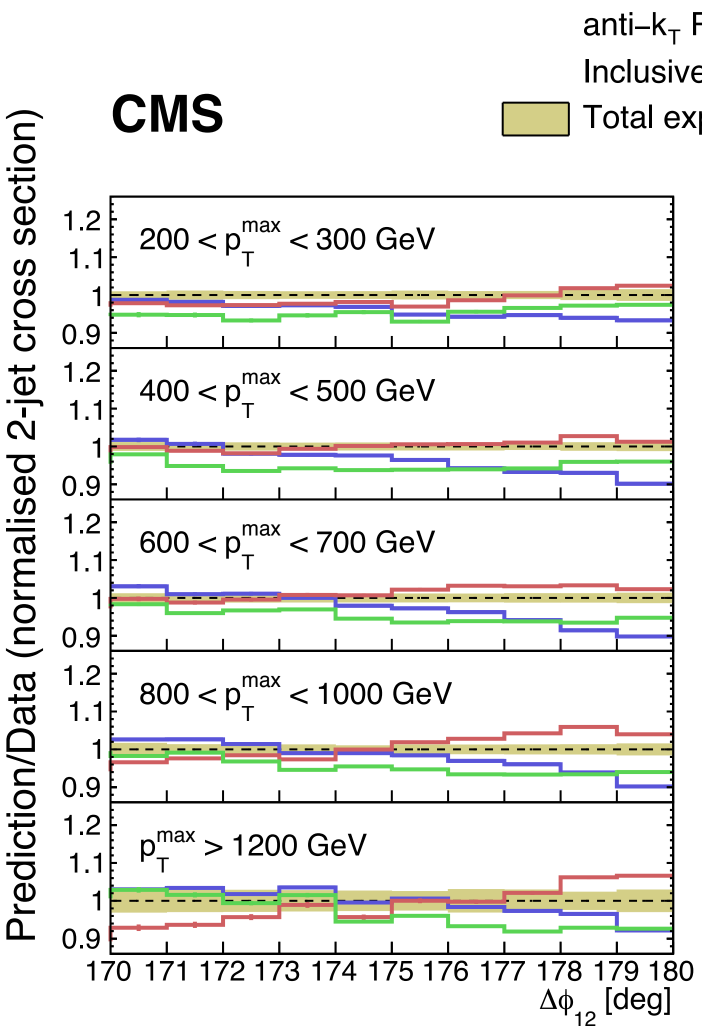

Inclusive 3-jet events

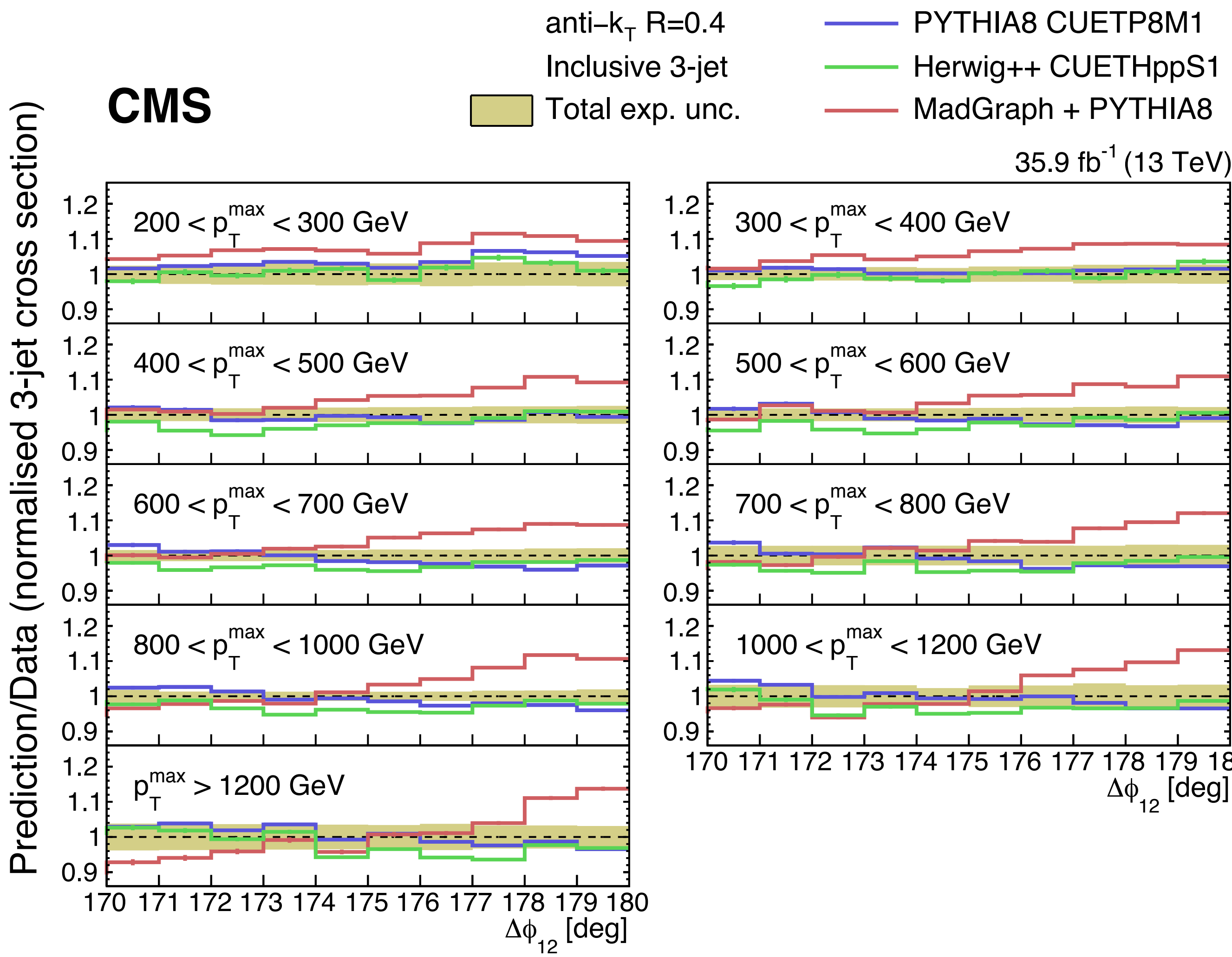

Azimuthal correlations in 2-, 3- and 4-jet events

Matrix element generator	Simulated diagrams	PDF set	Tune
PYTHIA 8.219 [9]	2→2 (LO)	NNPDF2.3LO [14, 15]	CUETP8M1 [13]
HERWIG++ 2.7.1 [10]	2→2 (LO)	CTEQ6L1 [16]	CUETHppS1 [13]
MADGRAPH5_aMC@NLO 2.3.3 [17, 18] + PYTHIA 8.219 [9]	2→2, 2→3, 2→4 (LO)	NNPDF2.3LO [14, 15]	CUETP8M1 [13]
POWHEG V2_Sep2016 [20–22] + PYTHIA 8.219 [9]	2→2 (NLO), 2→3 (LO)	NNPDF3.0NLO [28]	CUETP8M1 [13]
POWHEG V2_Sep2016 [20–22] + PYTHIA 8.219 [9]	2→3 (NLO), 2→4 (LO)	NNPDF3.0NLO [28]	CUETP8M1 [13]
POWHEG V2_Sep2016 [20–22] + HERWIG++ 2.7.1 [10]	2→2 (NLO), 2→3 (LO)	NNPDF3.0NLO [28]	CUETHppS1 [13]
HERWIG 7.0.4 [23]	2→2 (NLO), 2→3 (LO)	MMHT2014 [29]	H7-UE-MMHT [23]

Azimuthal correlations in 2-, 3- and 4-jet events

Measurement as a function of the minimum azimuthal angle between any of the 3 or 4 leading jets ($\Delta\phi_{2j}^{min}$)

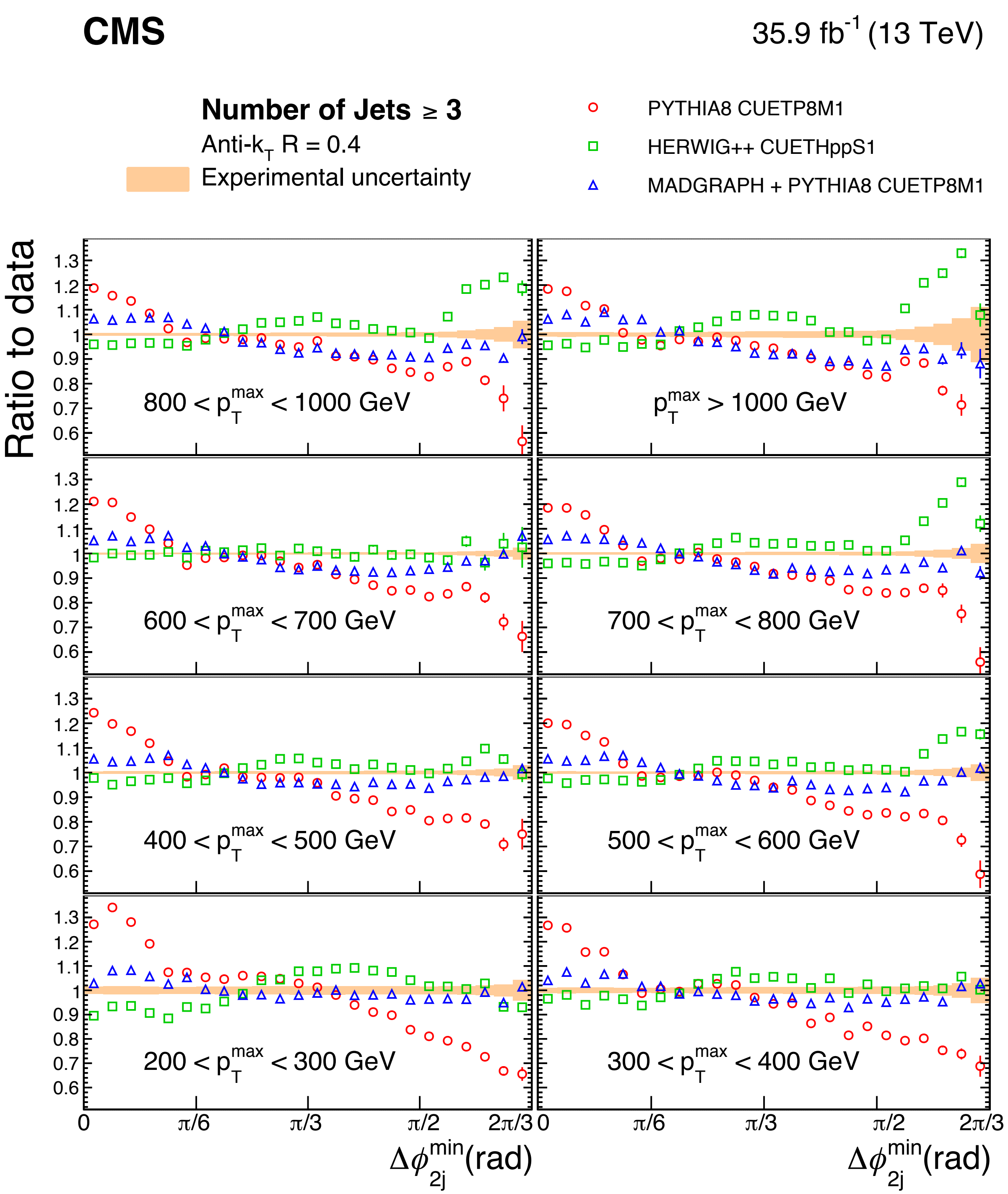

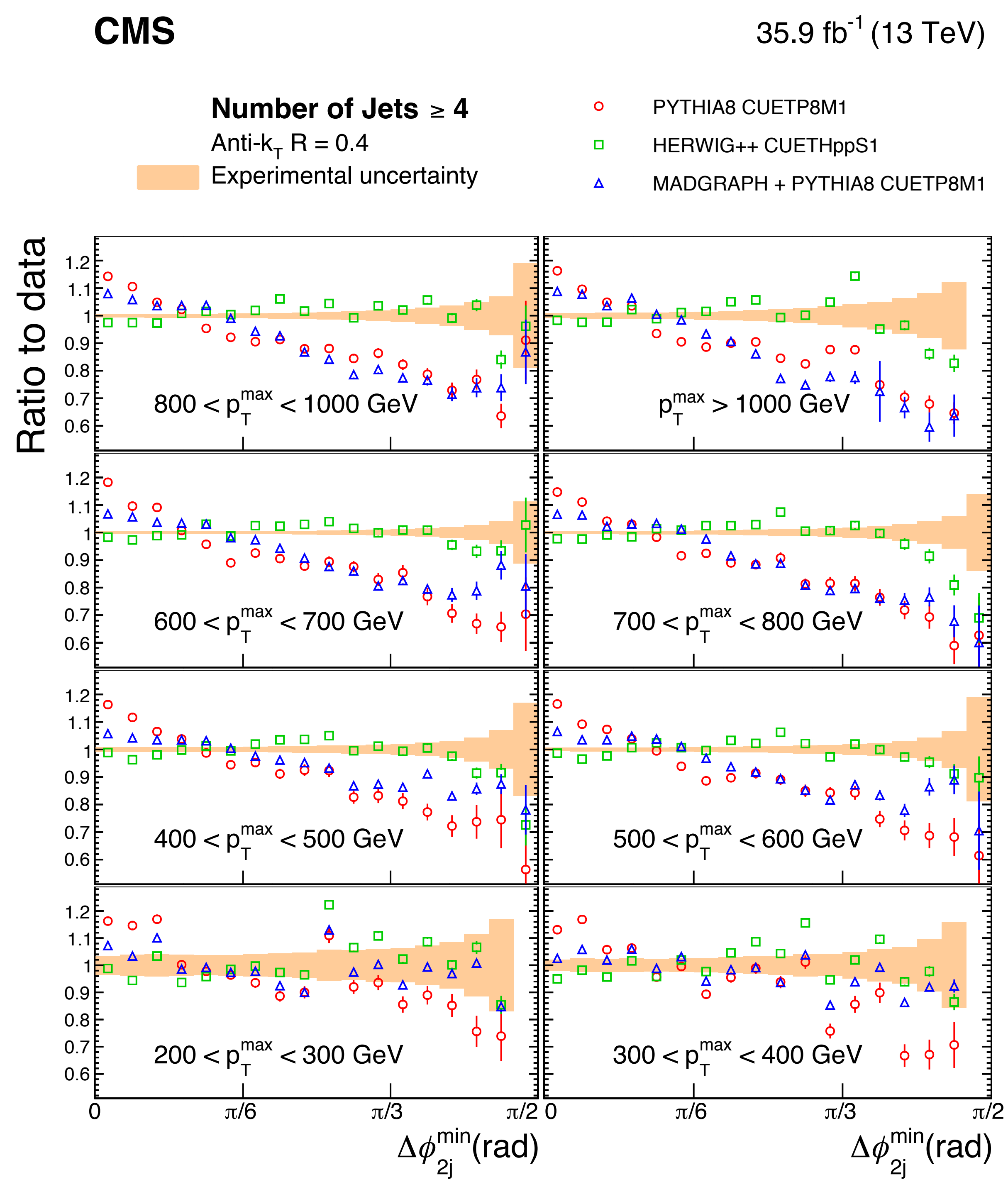

Event shape variables in multijet final states

Total jet broadening

Event divided into upper (U) and lower region (L) U: $\vec{p}_{T,i} \cdot \hat{n}_T > 0$ L: $\vec{p}_{T,i} \cdot \hat{n}_T < 0$

$$B_X \equiv \frac{1}{2p_T} \sum_{i \in X} p_{T,i} \sqrt{(\eta_i - \eta_X)^2 + (\phi_i - \phi_X)^2} \text{ where X= U, L}$$

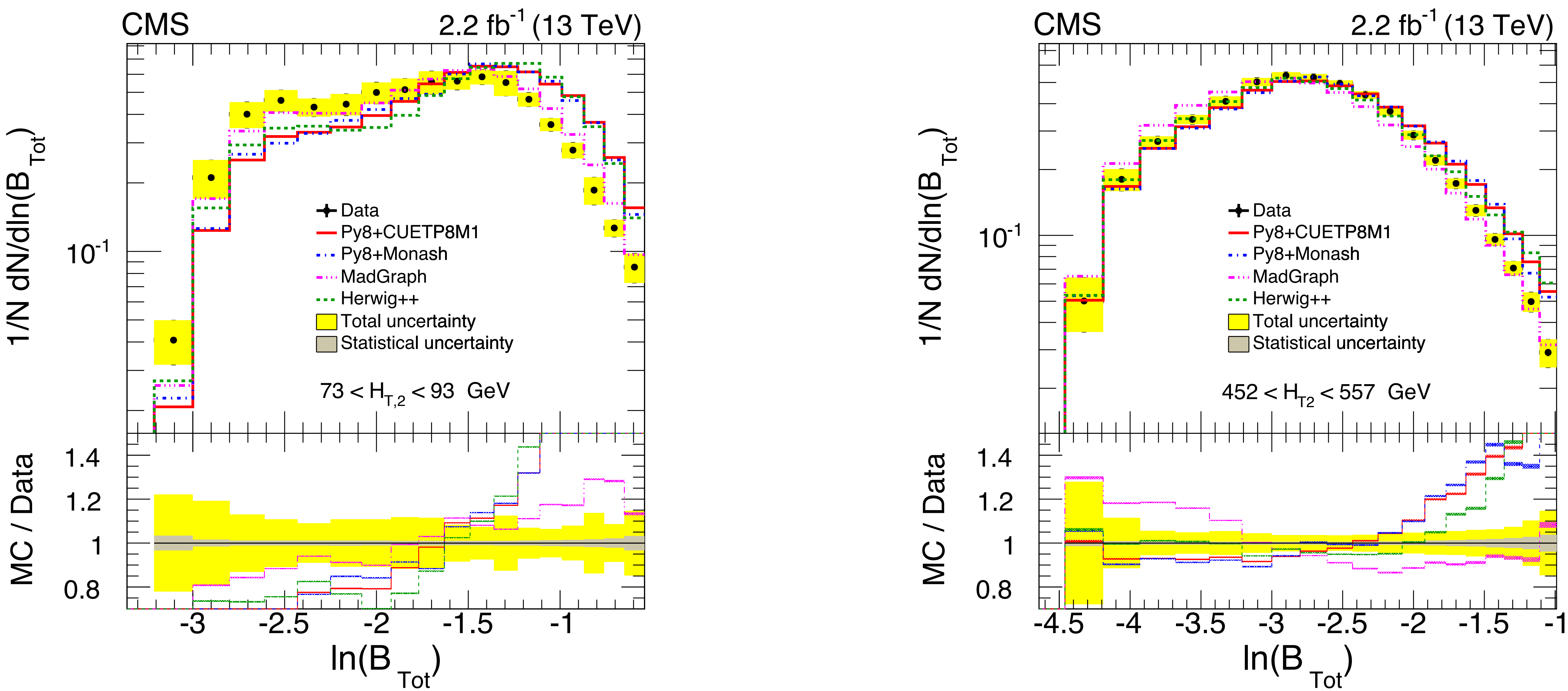

Both Herwig and Madgraph are in better agreement with the data than Pythia8

Better treatment of energy flow out of the transverse plane

Event shape variables in multijet final states

Total jet mass

$$\rho_X \equiv \frac{M_X^2}{P^2} \quad \text{where X= U, L}$$

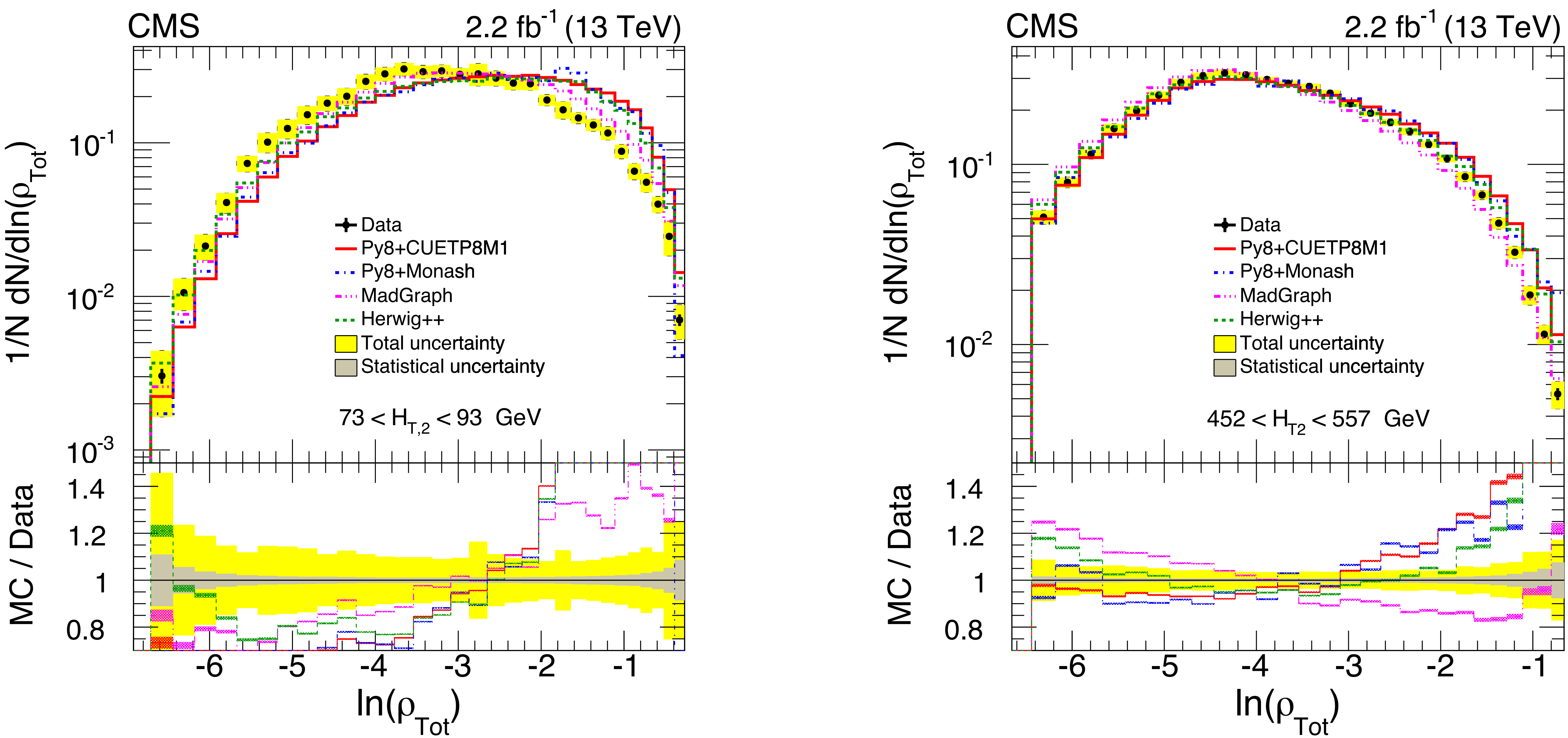

Both Herwig and Madgraph are in better agreement with the data than Pythia8
Better treatment of energy flow out of the transverse plane

Dijet azimuthal decorrelation

$$R_{\Delta\phi} = \frac{\frac{d^2\sigma_{\text{dijet}}(\Delta\phi_{\text{dijet}}<\Delta\phi_{\max})}{dH_T\,dy^*}}{\frac{d^2\sigma_{\text{dijet}}(\text{inclusive})}{dH_T\,dy^*}}$$

Quantity	Value
H_T bin boundaries (in TeV)	0.45, 0.6, 0.75, 0.9, 1.1, 1.4, 1.8, 2.2, 2.7, 4.0
y^* regions	0.0–0.5, 0.5–1.0, 1.0–2.0
$\Delta\phi_{\max}$ values	$7\pi/8$, $5\pi/6$, $3\pi/4$, $2\pi/3$

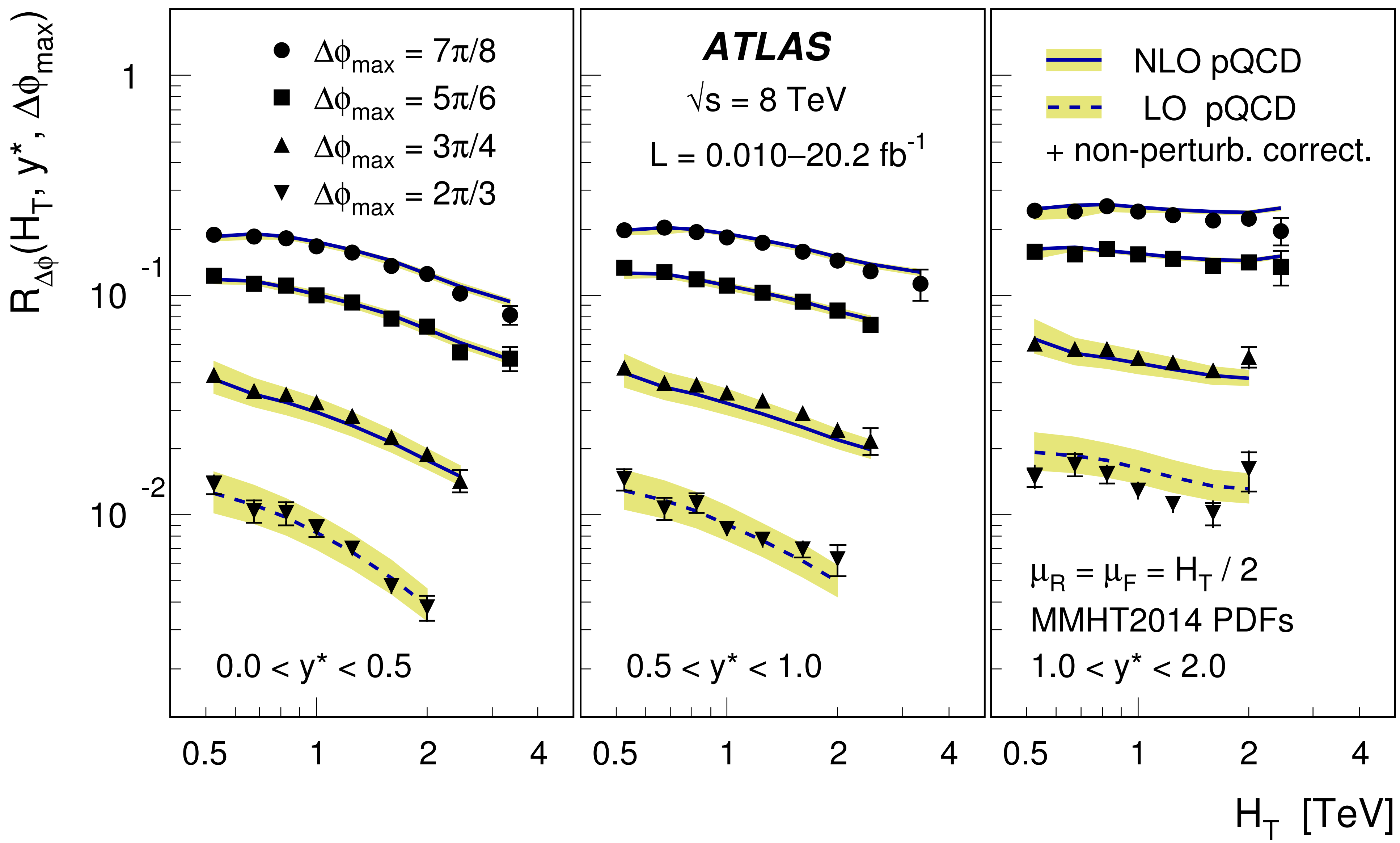

Measurement of the jet substructure observables

Dijet selection

2 large-R jets with $p_T > 200$ GeV
Leading jet $p_T > 450$ GeV and $|\eta| < 1.5$
Leptons veto

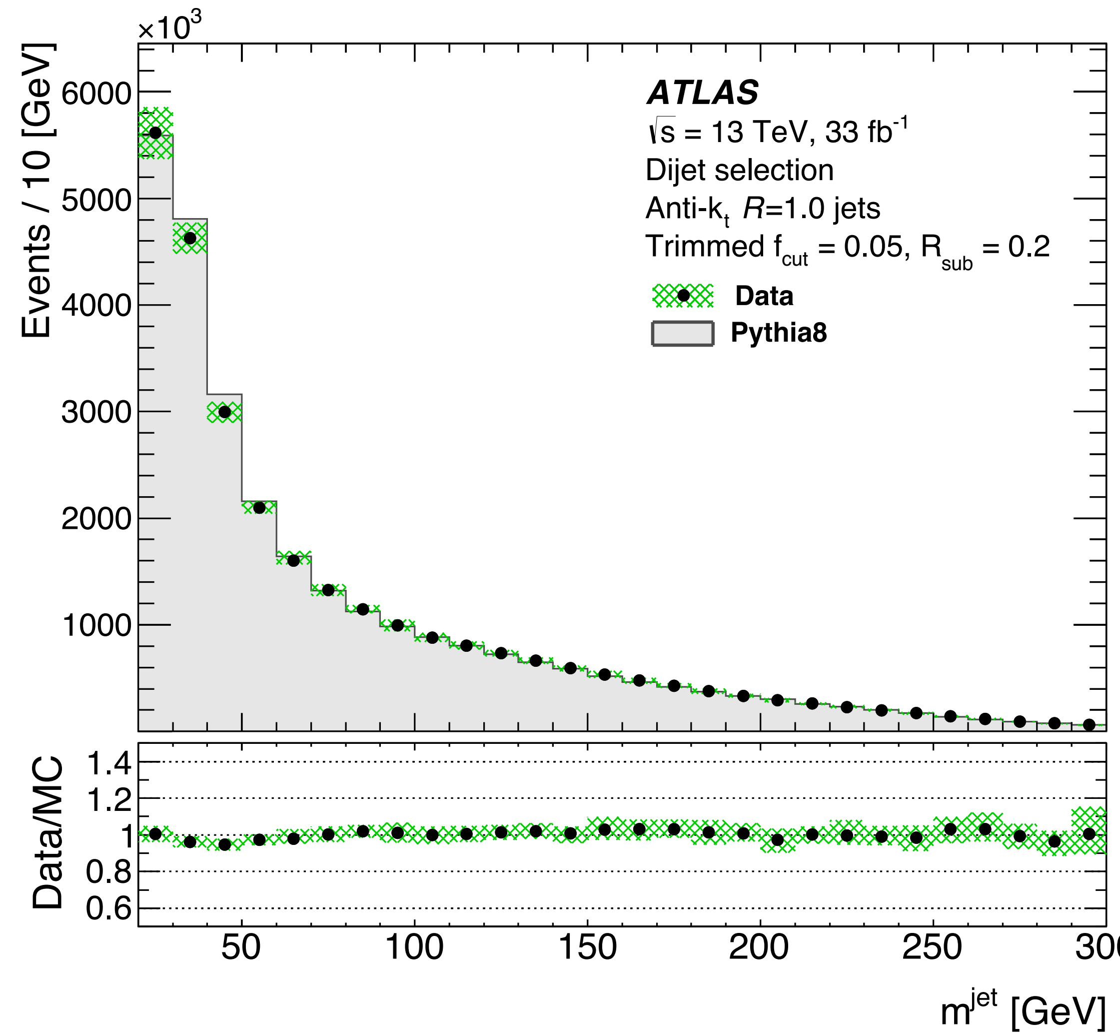

Measurement of the jet substructure observables

W and top selection

Top and W selections:	Detector level	Particle level
Exactly one muon	$p_T > 30$ GeV $\lvert\eta\rvert < 2.5$ $\lvert z_0 \sin(\theta)\rvert < 0.5$ mm and $\lvert d_0/\sigma(d_0)\rvert < 3$	$p_T > 30$ GeV $\lvert\eta\rvert < 2.5$
Anti-k_t $R = 0.4$ jets	$p_T > 25$ GeV $\lvert\eta\rvert < 4.4$ JVT output > 0.5 (if $p_T < 60$ GeV)	$p_T > 25$ GeV $\lvert\eta\rvert < 4.4$
Muon isolation criteria	If $\Delta R(\mu, \text{jet}) < 0.04 + 10$ GeV $/p_{T,\mu}$: muon is removed, so the event is discarded	None
E_T^{miss}, m_T^W	$E_T^{miss} > 20$ GeV , $E_T^{miss} + m_T^W > 60$ GeV	
Leptonic top	At least one small-radius jet with $0.4 < \Delta R(\mu, \text{jet}) < 1.5$	
Top selection:		
Leading-p_T trimmed anti-k_t $R = 1.0$ jet	$\lvert\eta\rvert < 1.5$, $p_T > 350$ GeV , mass > 140 GeV $\Delta R(\text{large-radius jet}, b\text{-tagged jet}) < 1$ $\Delta\phi(\mu, \text{large-radius jet}) > 2.3$	
W selection:		
Leading-p_T trimmed anti-k_t $R = 1.0$ jet	$\lvert\eta\rvert < 1.5$, $p_T > 200$ GeV , mass > 60 GeV and mass < 100 GeV $1 < \Delta R(\text{large-radius jet}, b\text{-tagged jet}) < 1.8$ $\Delta\phi(\mu, \text{large-radius jet}) > 2.3$	

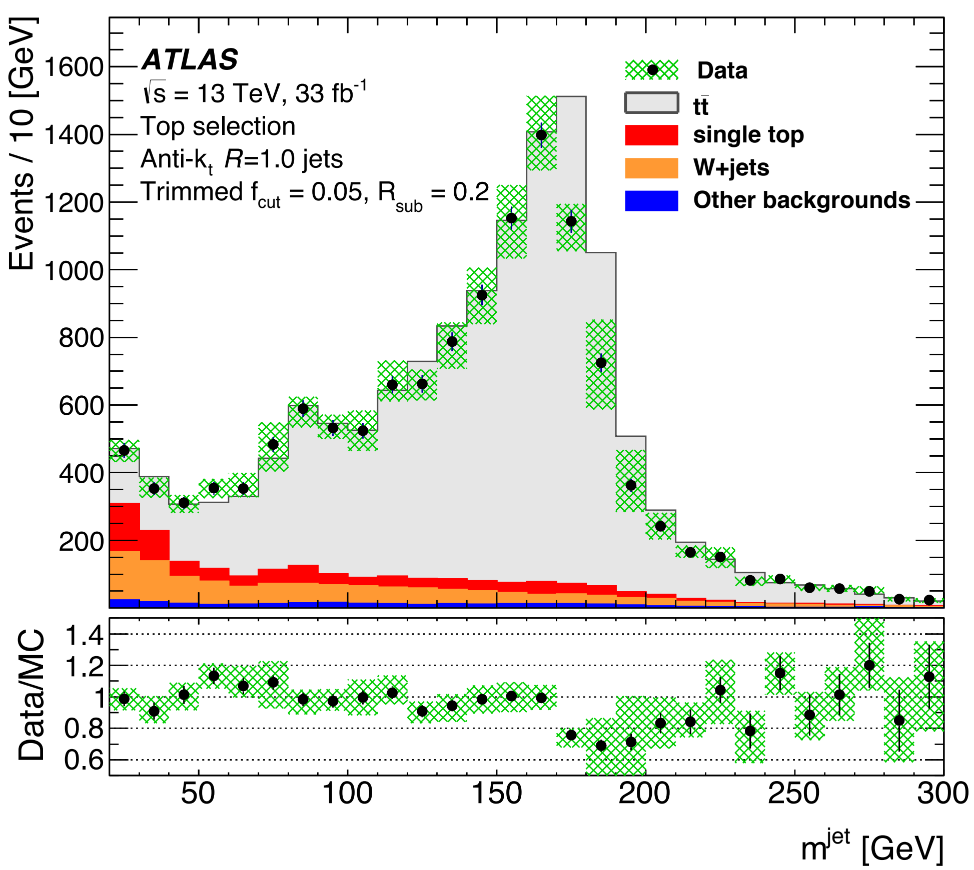

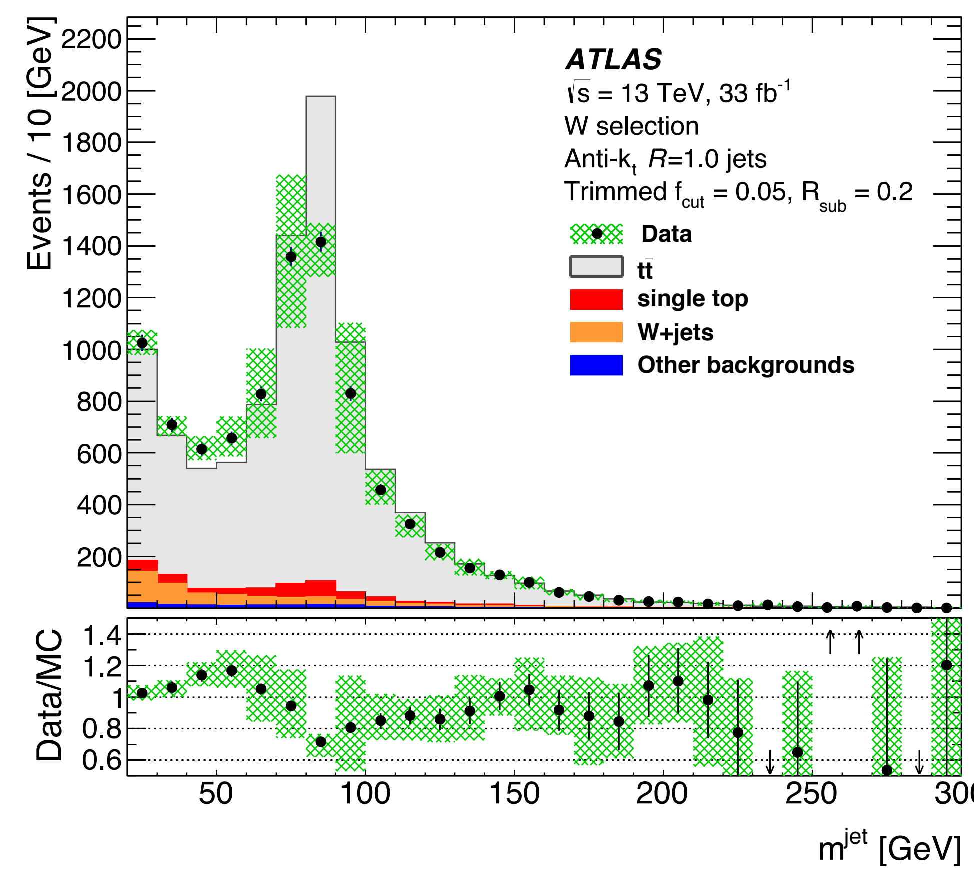

Gluon splitting into $b\bar{b}$

Signed impact parameter significance

$$s_{d_0} = s_j |d_0| / \sigma(d_0)$$

	$\Delta R(b,b)$	$\Delta\theta_{\mathrm{ppg,gbb}}$	$z(p_{\mathrm{T}})$	$\log(m_{bb}/p_{\mathrm{T}})$
Calorimeter jet energy	2–3%	2–3%	2–6%	2–4%
Flavor tagging	<1%	<1%	<1%	<1%
Tracking	1–2%	1–2%	2–4%	1–2%
Background fit	1%	1%	1–2%	2%
Unfolding method	2–3%	2%	2–4%	2–5%
Theoretical modeling	3–10%	2–13%	3–10%	4–11%
Statistical	1%	1%	2%	1%
Total	3–10%	3–10%	3–14%	4–12%

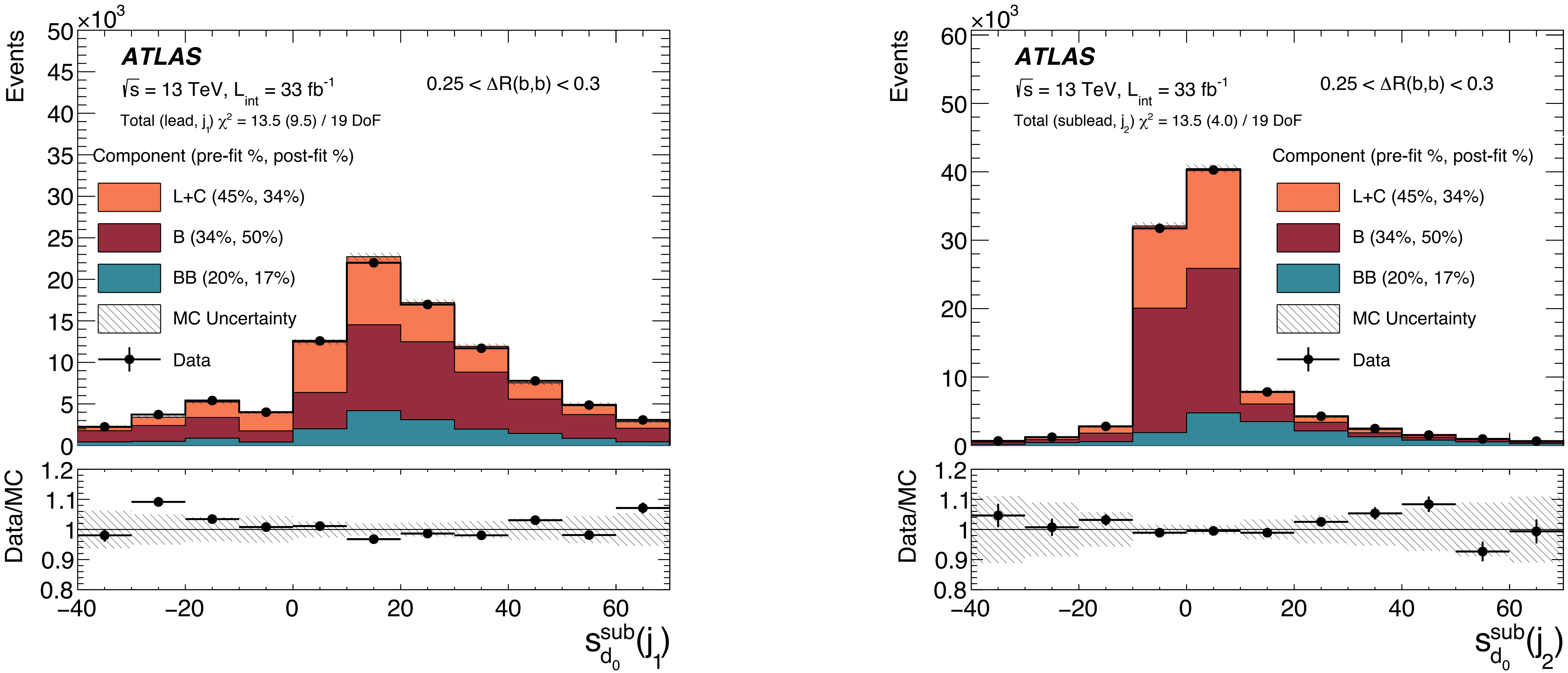

Jet mass cross section in dijet events

$p_T > 200$ GeV and $|\eta| < 2.4$

$(p_{T,1} - p_{T,2})/(p_{T,1} + p_{T,2}) < 0.3$ and $\Delta\phi > \pi/2$ to reduce the number of jets from detector noise and ensure a high-purity dijet like sample

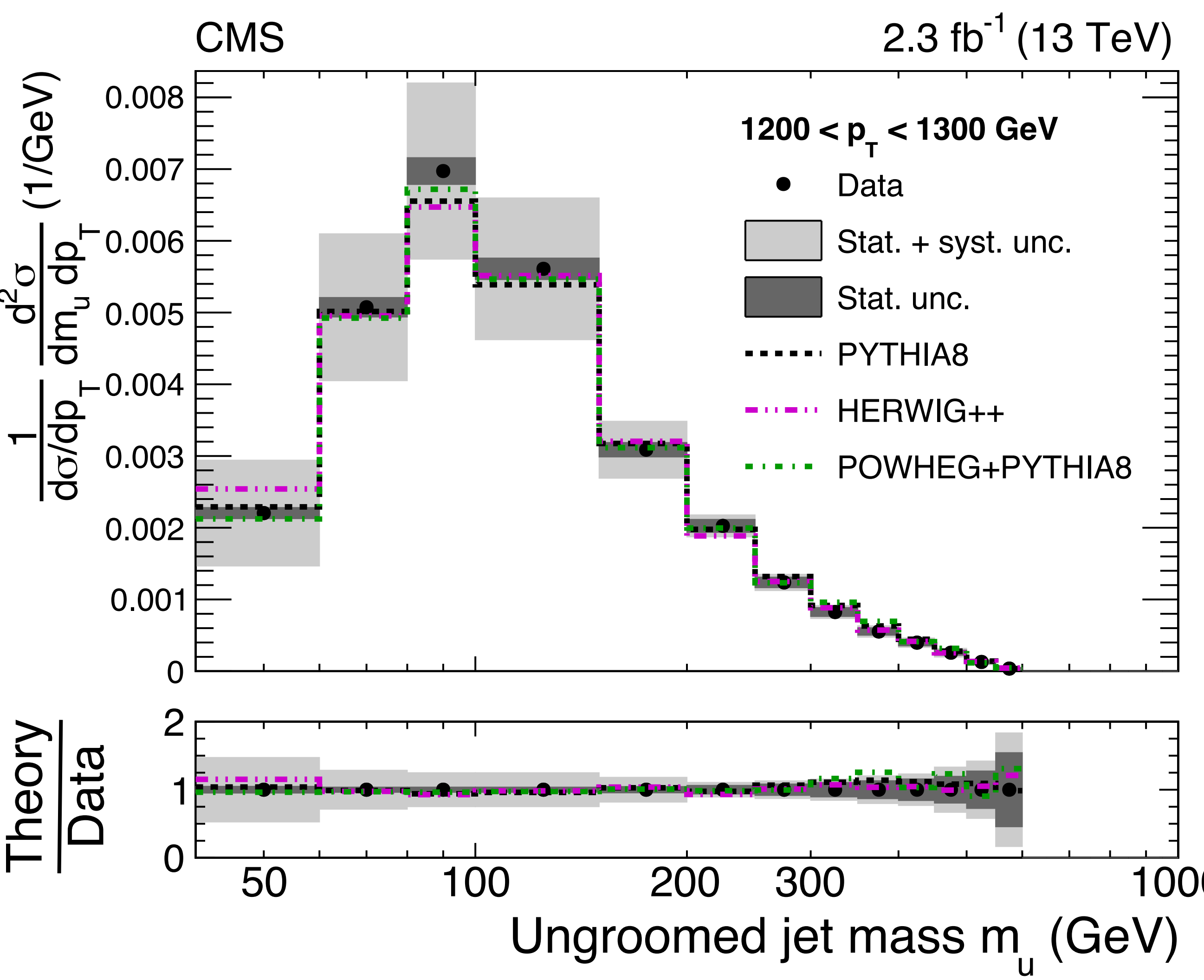

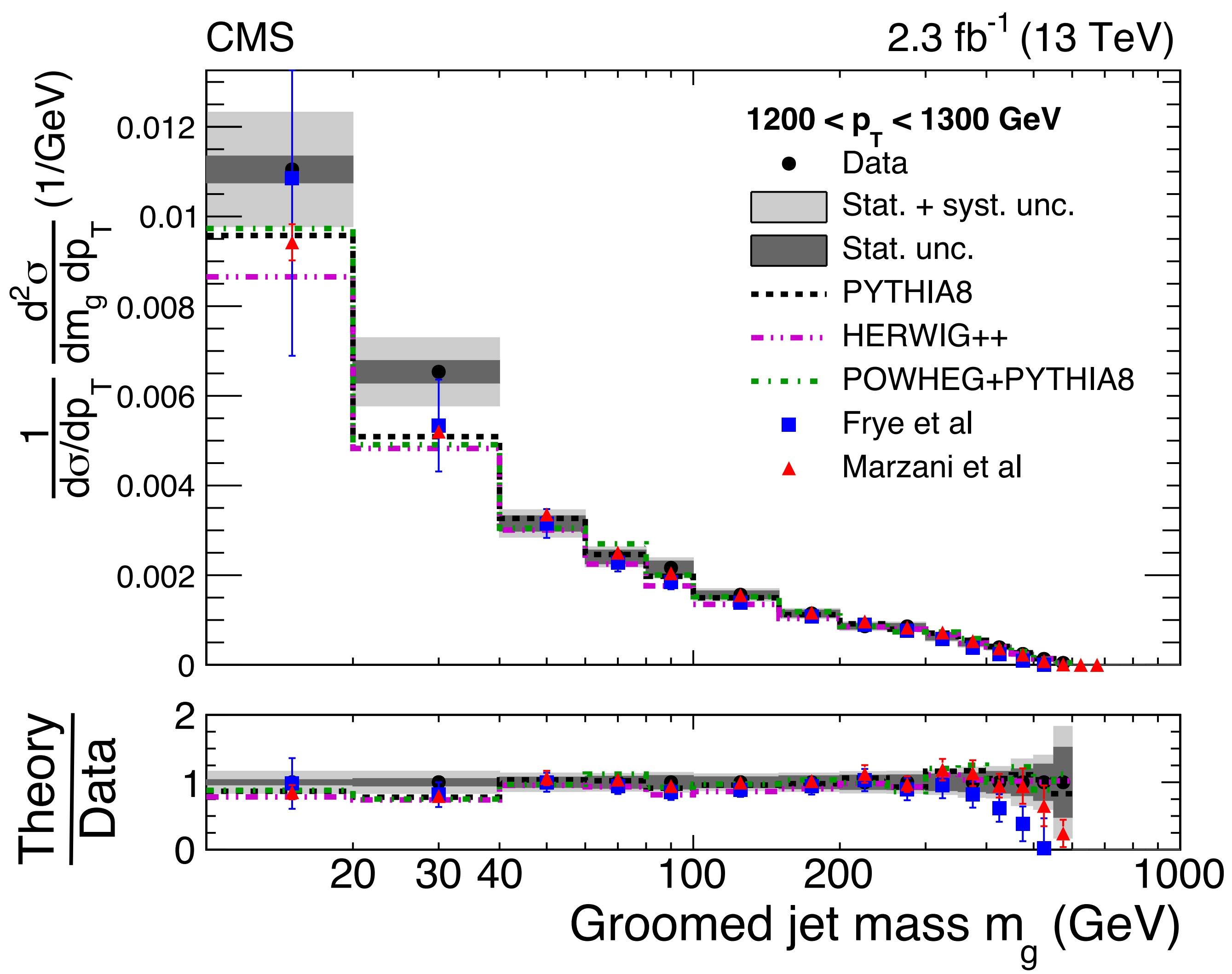

Photon isolation

E_T^{iso} is computed summing the transverse energy of clusters of calorimeter cells in a cone of radius 0.4, excluding the contribution from the photon.

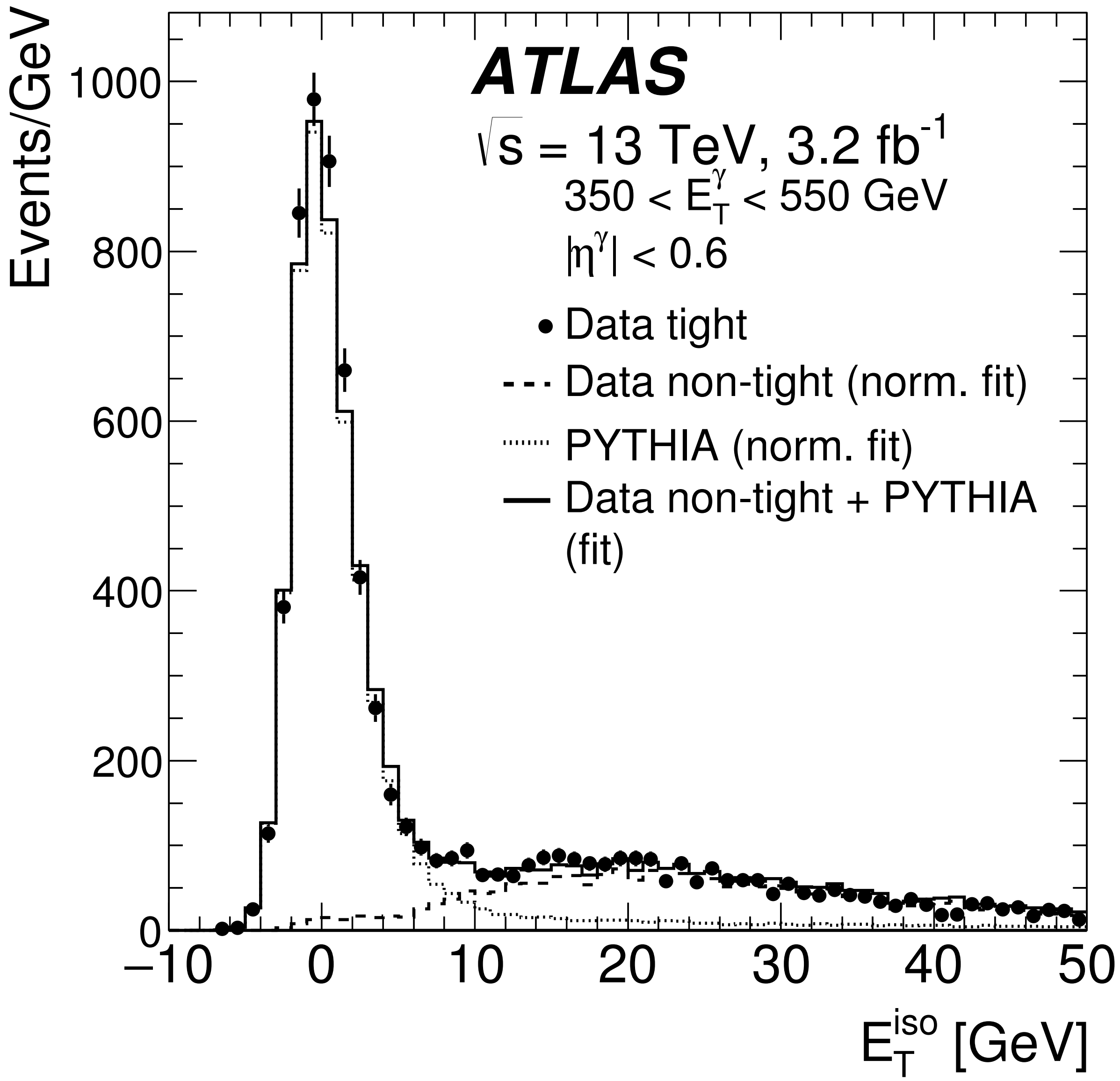

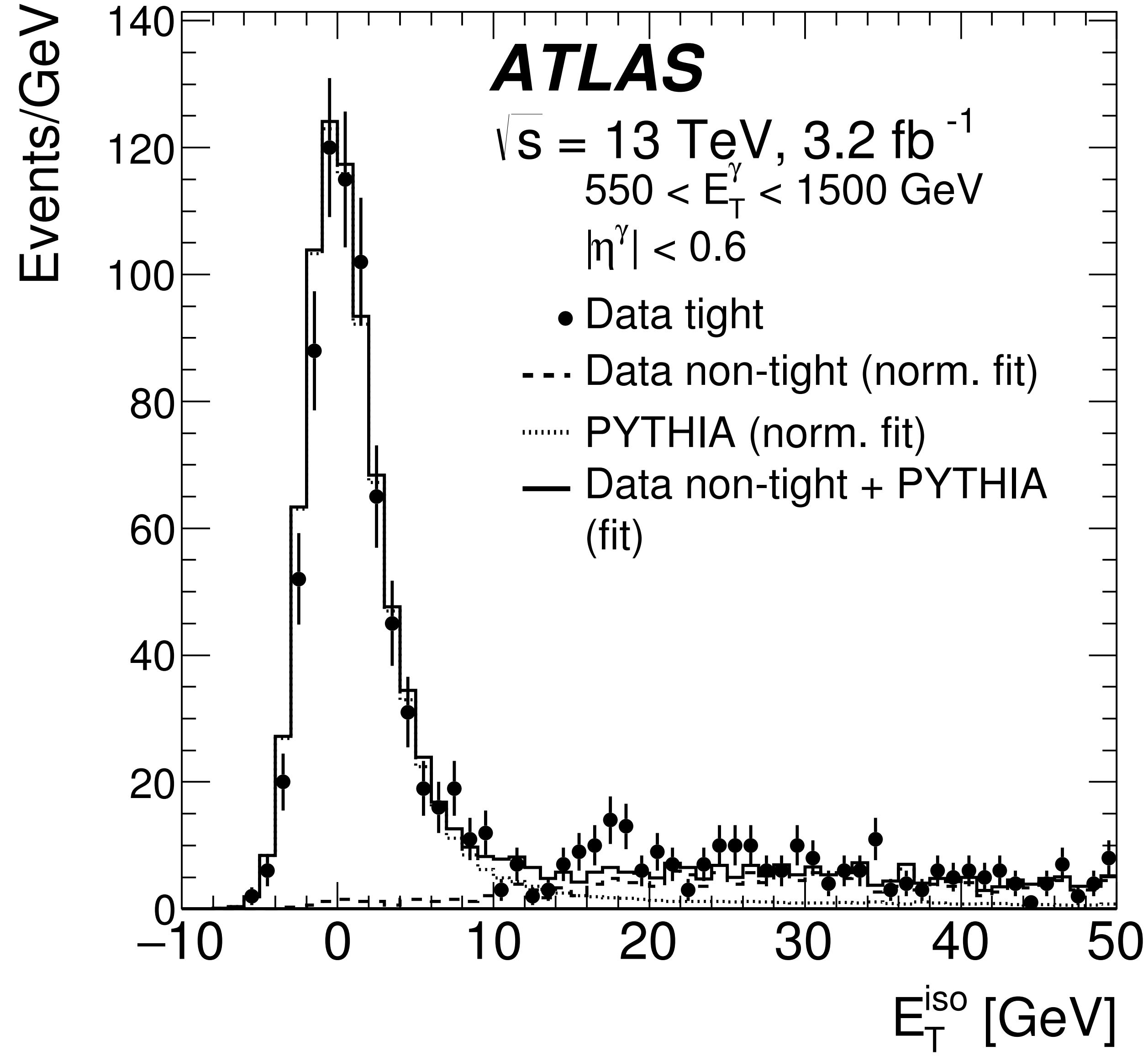

Additional cuts

Selection of unbiased region to measure $|\cos\theta^*|$ and $m^{\gamma-jet}$ cross sections:

$$|\eta^\gamma + y^{jet}| < 2.37 \qquad |\cos\theta^*| < 0.83 \qquad m^{\gamma-jet} > 450\ \mathrm{GeV}$$

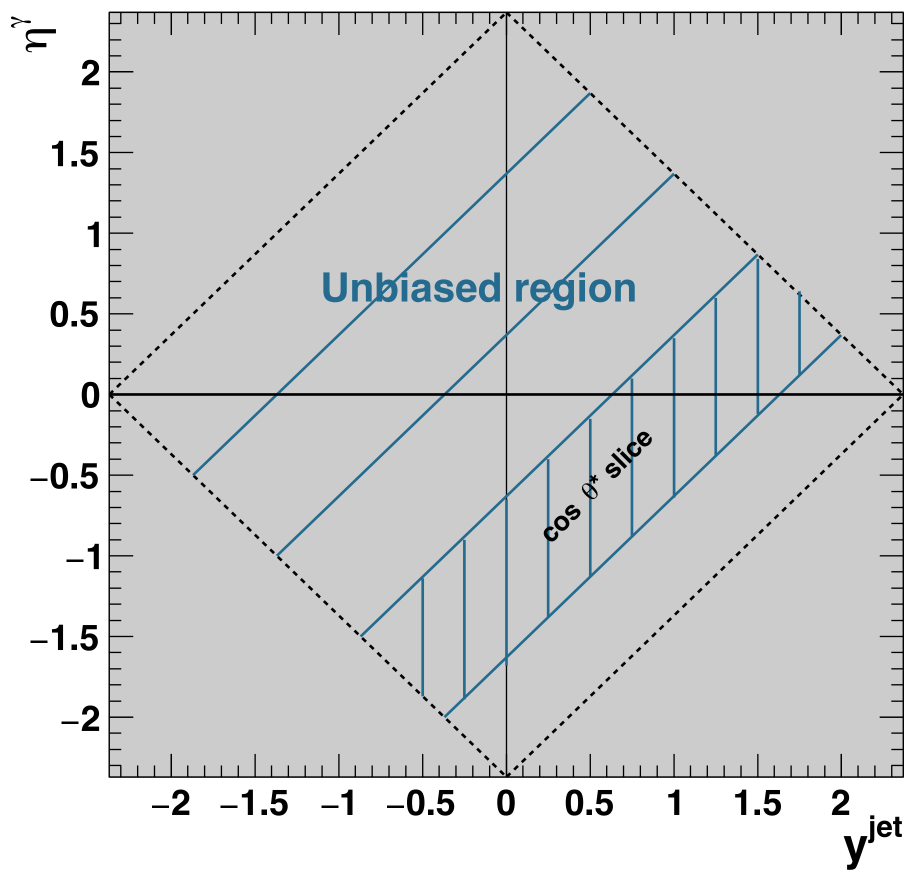

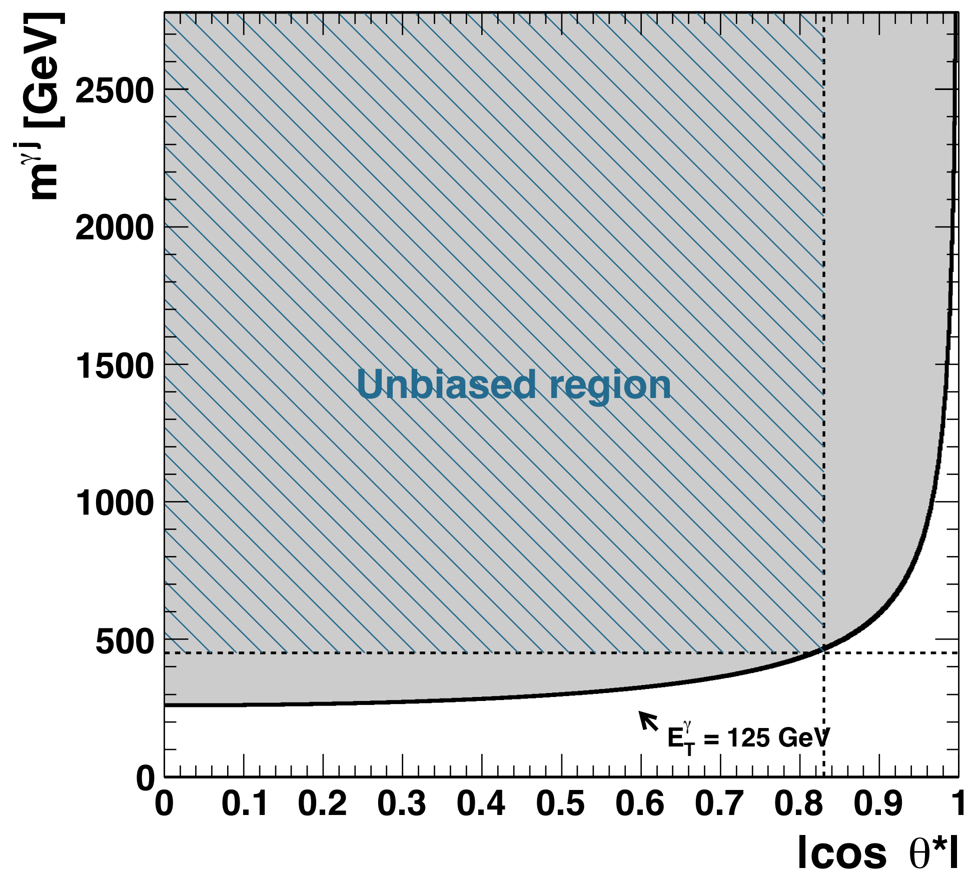

The first two requirements avoid the bias induced by the cut on $|\eta^\gamma|$ and y^{jet}. The third requirement avoids the bias due to the E_T^γ cut in the ($|\cos\theta^*| - m^{\gamma-jet}$) plane.

Photon + jet at 13 TeV

Requirements on photons
$E_T^{\gamma} > 125$ GeV, $\lvert\eta^{\gamma}\rvert < 2.37$ (excluding $1.37 < \lvert\eta^{\gamma}\rvert < 1.56$)
$E_T^{\text{iso}} < 4.2 \cdot 10^{-3} \cdot E_T^{\gamma} + 10$ GeV
Requirements on jets
anti-k_t algorithm with $R = 0.4$
the leading jet within $\lvert y^{\text{jet}}\rvert < 2.37$ and $\Delta R^{\gamma-\text{jet}} > 0.8$ is selected
$p_T^{\text{jet-lead}} > 100$ GeV
UE subtraction using $k_{\perp}$ algorithm with $R = 0.5$ (cf. Section ??)
Additional requirements for $d\sigma/dm^{\gamma-\text{jet}}$ and $d\sigma/d\lvert\cos\theta^*\rvert$
$\lvert\eta^{\gamma} + y^{\text{jet-lead}}\rvert < 2.37$, $\lvert\cos\theta^*\rvert < 0.83$ and $m^{\gamma-\text{jet}} > 450$ GeV

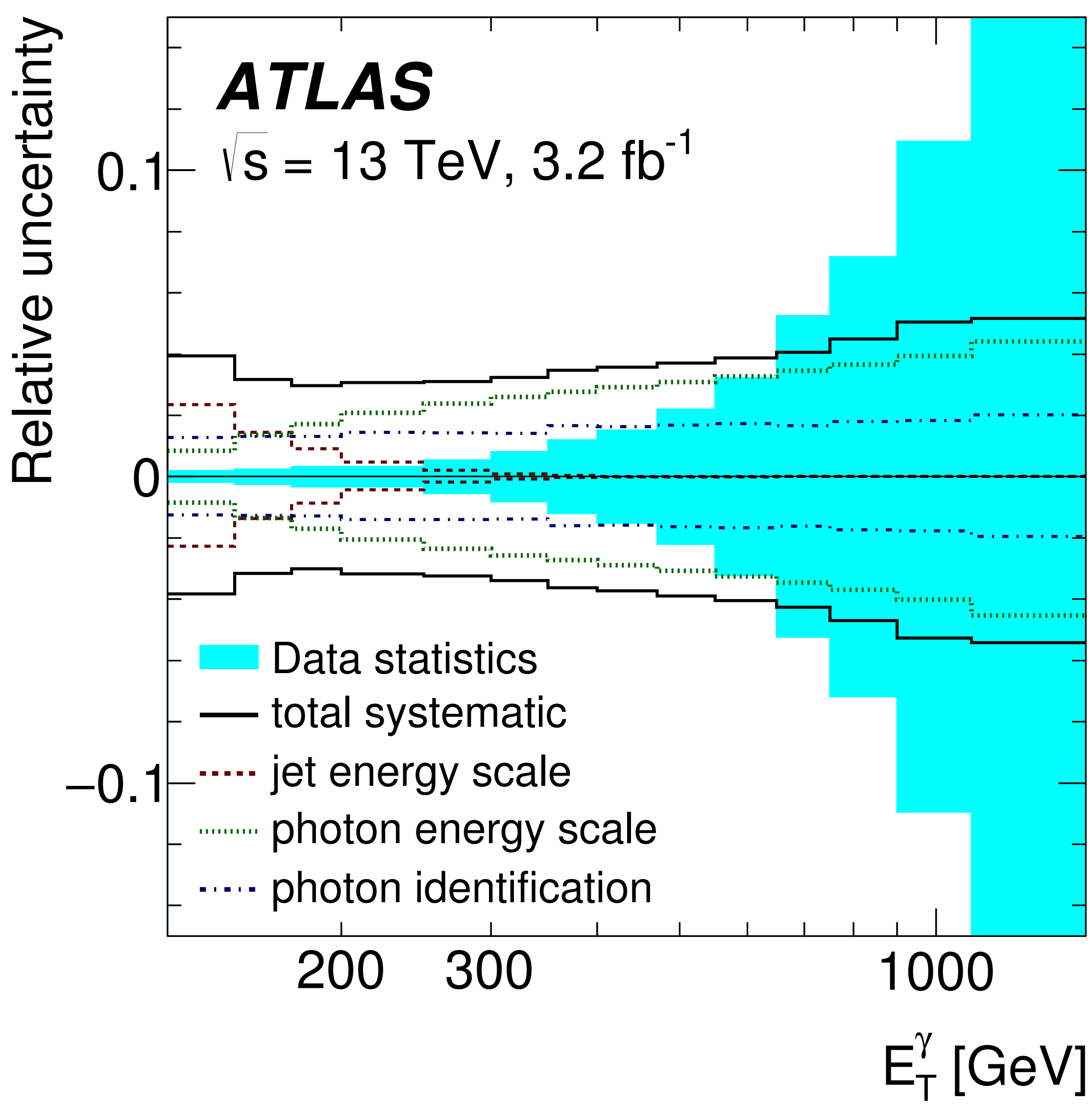

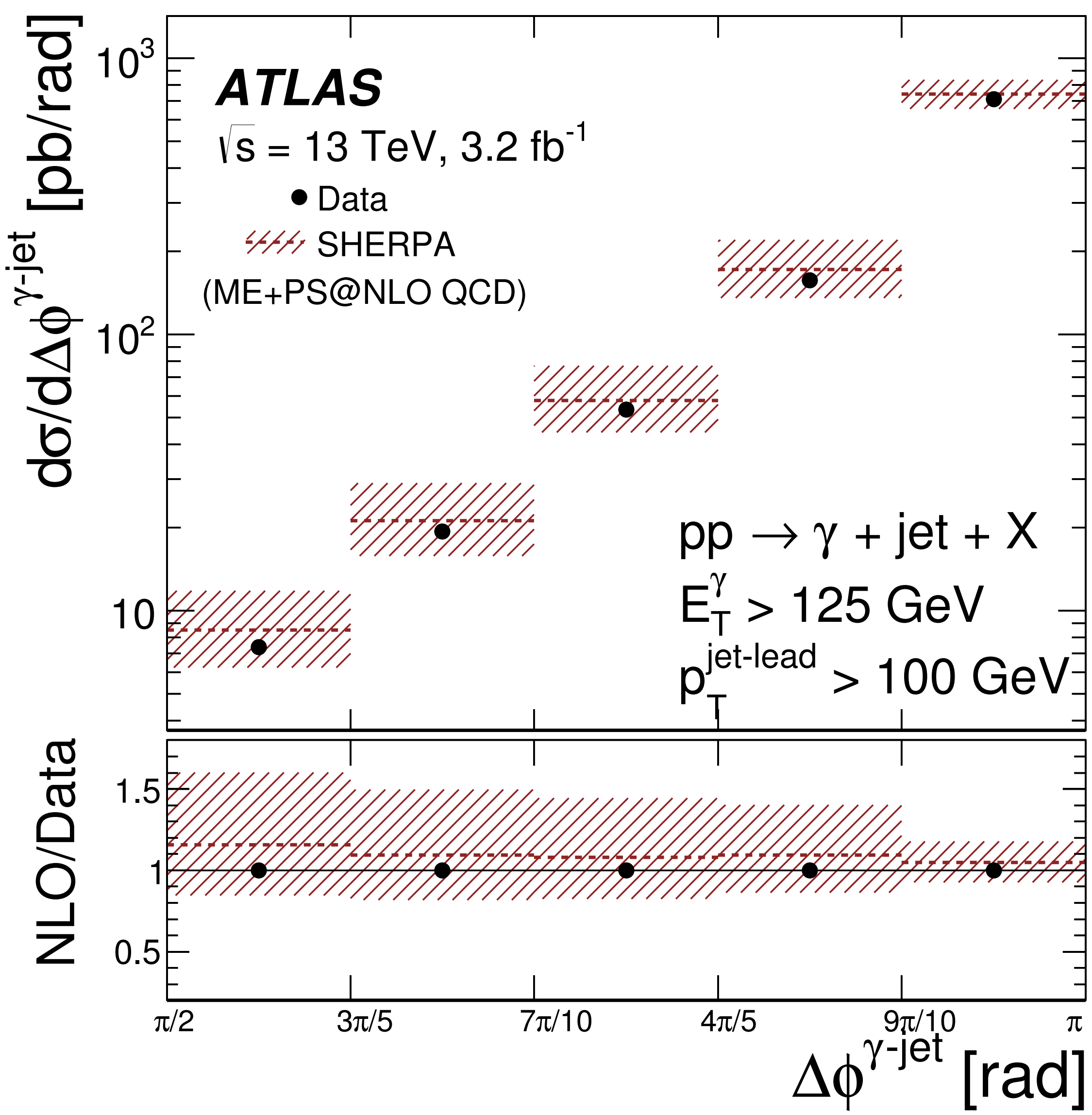

Ratio of photon cross sections at 8 and 13 TeV

- Assuming no correlation provides a conservative estimate and full correlation is used only when justified.
- The uncertainty arising from the γ energy scale is estimated by decomposing it into uncorrelated sources for both the 8 and 13 TeV measurements
- 22 individual components are then considered
- 20 of these components are common to both center-of-mass energies
- The remaining two components are specific to the 13 TeV measurement
- All the components are taken as fully correlated except for the uncertainty in the overall energy scale adjustment using $Z \rightarrow e^+e^-$ events, which for 2015 includes the effects of the changes in the configuration of the ATLAS detector, and the uncertainties specific to the 13 TeV measurement.
- The uncertainties due the γ energy resolution are treated as uncorrelated since they include the effects of pile-up, which was different in the 2012 and 2015 data-taking periods
- Other sources of uncertainty are treated as uncorrelated

Ratio of photon cross sections at 8 and 13 TeV

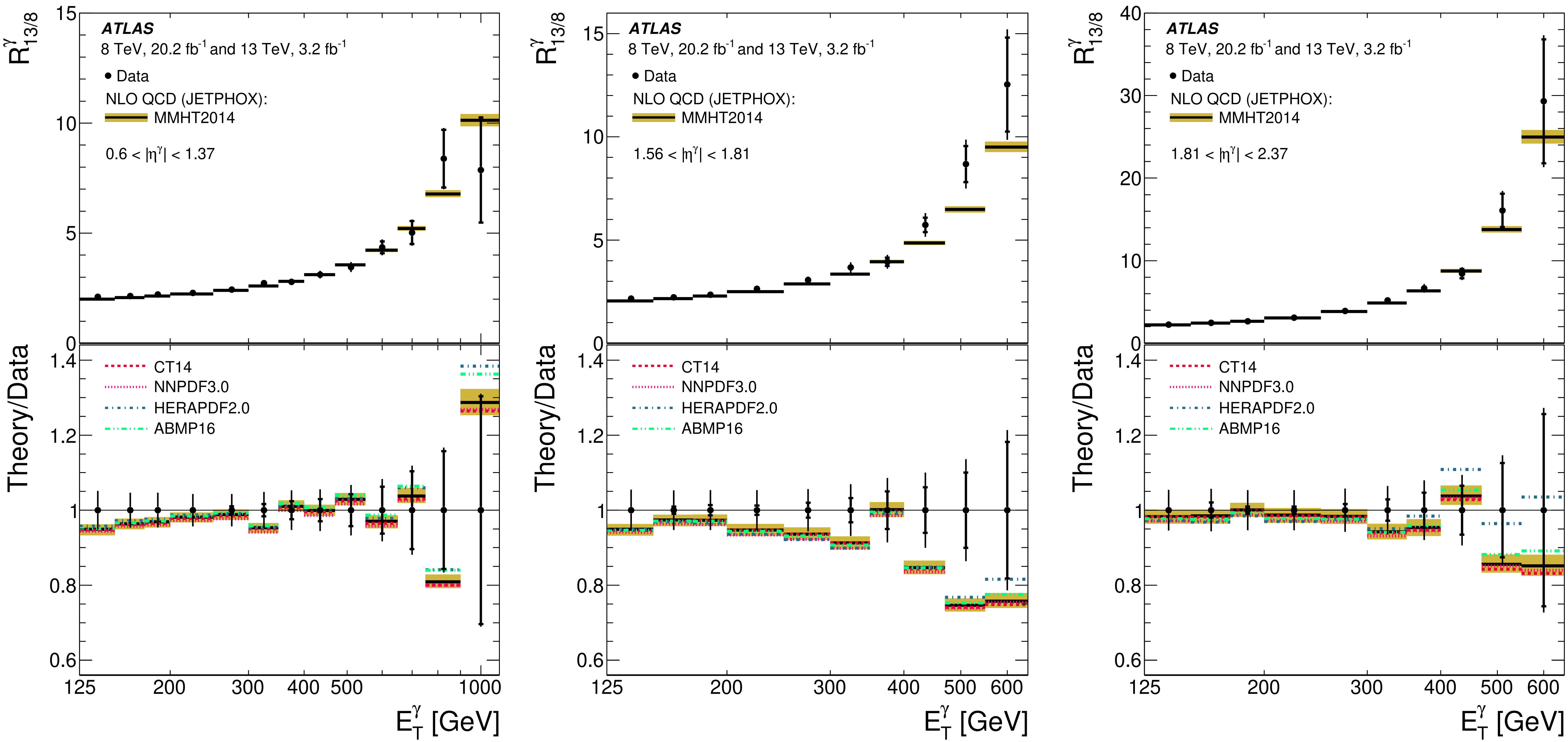

Inclusive photon and γ+ jet at 13 TeV

Inclusive (+jet) cross sections are measured as a function of E_{T}^{γ} and $|\eta^{\gamma}|$ (and $|y^{jet}|$)

Source	$\lvert y^{\gamma}\rvert < 0.8$	$0.8 < \lvert y^{\gamma}\rvert < 1.44$	$1.57 < \lvert y^{\gamma}\rvert < 2.1$	$2.1 < \lvert y^{\gamma}\rvert < 2.5$
Trigger efficiency	0.7–8.5	0.2–13.4	0.6–20.5	0.3–7.8
Selection efficiency	0.1–1.3	0.1–1.3	0.1–5.3	0.1–1.1
Data-to-MC scale factor	3.7	3.7	7.1	7.1
Template shape	0.6–5.0	0.1–10.2	0.5–4.9	0.6–16.2
Unfolding	3.8–5.5	1.2–4.1	2.0–8.5	2.3–10.3
Total w/o luminosity	5.4–12.0	5.9–18.2	8.2–26.9	8.6–21.7
Integrated luminosity		2.3		

Inclusive photon and γ+ jet at 13 TeV